



## Open Archive TOULOUSE Archive Ouverte (OATAO)

OATAO is an open access repository that collects the work of Toulouse researchers and makes it freely available over the web where possible.

This is an author-deposited version published in : <http://oatao.univ-toulouse.fr/>  
Eprints ID : 9949

**To link to this article** : DOI:10.1021/ie3011148  
URL : <http://dx.doi.org/10.1021/ie3011148>

**To cite this version** : Shen, Weifeng and Benyounes, Hassiba and Gerbaud, Vincent. *Extension of thermodynamic insights on batch extractive distillation to continuous operation. 1. Azeotropic mixtures with a heavy entrainer*. (2013) Industrial & Engineering Chemistry Research, vol. 52 (n° 12). pp. 4606-4622. ISSN 0888-5885

Any correspondence concerning this service should be sent to the repository administrator: [staff-oatao@listes-diff.inp-toulouse.fr](mailto:staff-oatao@listes-diff.inp-toulouse.fr)

# Extension of Thermodynamic Insights on Batch Extractive Distillation to Continuous Operation. 1. Azeotropic Mixtures with a Heavy Entrainer

Weifeng Shen,<sup>†,‡</sup> Hassiba Benyounes,<sup>§</sup> and Vincent Gerbaud<sup>\*,†,‡</sup>

<sup>†</sup>Université de Toulouse, INP, UPS, LGC (Laboratoire de Génie Chimique), 4 allée Emile Monso, F-31432 Toulouse Cedex 04, France

<sup>‡</sup>CNRS, LGC (Laboratoire de Génie Chimique), F-31432 Toulouse Cedex 04, France

<sup>§</sup>Laboratoire de Chimie Physique des Matériaux, Catalyse et Environnement, Université des Sciences et de la Technologie Oran (UST Oran), Oran, Algérie

**ABSTRACT:** We have studied the batch and continuous extractive distillation of minimum- and maximum-boiling azeotropic mixtures with a heavy entrainer. These systems exhibit class 1.0-1a and 1.0-2 ternary diagrams, each with two subcases depending on the location of the univolatility line. The feasible product and feasible ranges of the operating parameters reflux ratio ( $R$ ) and entrainer/feed flow rate ratio for continuous ( $F_E/F$ ) and batch ( $F_E/V$ ) operation were assessed. Class 1.0-1a processes allow the recovery of only one product because of the location of the univolatility line above a minimum value of the entrainer/feed flow rate ratio for both batch and continuous processes. A minimum reflux ratio  $R$  also exists. For an identical target purity, the minimum feed ratio is higher for the continuous process than for the batch process, for the continuous process where stricter feasible conditions arise because the composition profile of the stripping section must intersect that of the extractive section. Class 1.0-2 mixtures allow either A or B to be obtained as a product, depending on the feed location. Then, the univolatility line location sets limiting values for either the maximum or minimum of the feed ratio  $F_E/F$ . Again, the feasible range of operating parameters for the continuous process is smaller than that for the batch process. Entrainer comparison in terms of minimum reflux ratio and minimum entrainer/feed ratio is enabled by the proposed methodology.

## 1. INTRODUCTION

Even though distillation is the leading process for the purification of liquid mixtures, distillation research is still a challenging issue because many process improvements are possible. To reduce the high energy consumption of distillation systems, various alternatives have been proposed: highly integrated distillation columns (HIDIC),<sup>1–4</sup> vapor recompression columns,<sup>5</sup> and Petlyuk-like columns.<sup>6–9</sup> Distillation research is also fueled by the search for new operating modes or process alternatives that would allow for the separation of more nonideal mixtures, azeotropic mixtures, and low-relative-volatility mixtures. For ternary mixtures, only 16 of the 26 theoretically possible classes according to Serafimov's classification scheme have been matched by real ternary mixtures.<sup>10,11</sup> Recently, Reshetov and Kravchenko reported statistics for zeotropic mixture subclasses, distinguished by the occurrence and location of univolatility curves.<sup>12</sup>

To separate nonideal mixtures in continuous operation, pressure-swing, azeotropic, and extractive distillation processes are the most common methods used in industry and are well described in numerous textbooks.<sup>13–15</sup> Since the 1990s, studies of batch distillation processes have added new insights into both batch and continuous distillation operation and assisted the selection of proper feed compositions in continuous operation. For example, a feasibility criterion based on thermodynamic properties of ternary diagrams can now help design pressure-swing batch distillation process.<sup>16–20</sup> Exhaustive feasibility rules for the batch azeotropic distillation of

homogeneous<sup>21</sup> and heterogeneous<sup>22–25</sup> mixtures have increased the number of mixture classes suitable for azeotropic batch distillation. Novel operating modes such as double columns have been proposed.<sup>26</sup>

Regarding extractive distillation, studies involving continuous operating mode have relied for decades on a simple feasibility rule:<sup>27–29</sup> For the separation of a minimum- (maximum-) boiling azeotropic mixture A–B, one should add a heavy (light) entrainer E that forms no new azeotrope. The corresponding ternary mixture A–B–E belongs to class 1.0-1a,<sup>11</sup> which accounts for 21.6% of all azeotropic ternary mixtures.<sup>10</sup> A general feasibility criterion for extractive distillation shows that mixtures belonging to classes 1.0-2 and 1.0-1b are suited for batch extractive distillation, enabling the use of heavy, light, or intermediate entrainers for the separation of minimum- or maximum-boiling azeotropic mixtures or of low-relative-volatility mixtures.<sup>30–33</sup> The use of entrainers forming new azeotropes is also a possibility for batch extractive distillation for classes 2.0-1, 2.0-2a, 2.0-2b, and 2.0-2c.<sup>34</sup> The total occurrence of suitable ternary mixtures classes for extractive distillation in batch operating mode now reaches 53%.

In the present work, we studied how some of the new feasibility rules illustrated for batch extractive distillation are indeed valid for continuous distillation, enabling feasible composition regions to be proposed and hinting at possible limiting values for the entrainer/feed flow rate ratio and reflux

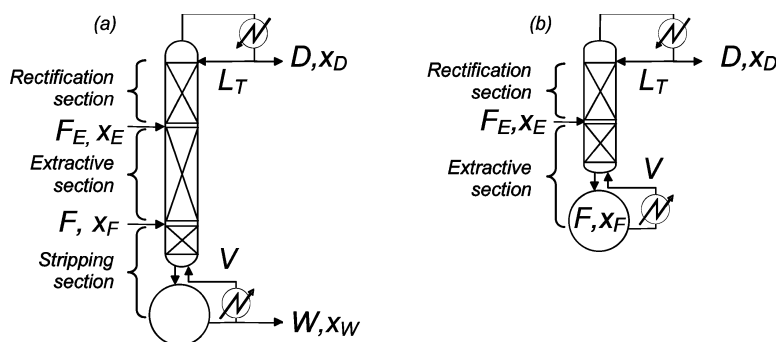


Figure 1. Configurations of extractive distillation columns: (a) continuous, (b) batch.

ratio, defining feasible ranges for a given entrainer. We focus in this first part of this article on the separation of minimum- and maximum-boiling azeotropic mixtures with a heavy entrainer that forms no new azeotrope, which correspond to classes 1.0-1a (21.6% occurrence) and 1.0-2 (8.5% occurrence), respectively. The class 1.0-1a case is often studied in continuous operation, but not under the thermodynamic insights of the general feasibility criterion for extractive distillation that covers all possible product occurrences. No detailed study of class 1.0-2 continuous extractive distillation has been reported in the literature.

## 2. STATE OF THE ART

Extractive distillation relies on the addition of an entrainer E at a location other than that of the main feed, whereas both the entrainer and main feed are fed together for azeotropic distillation. Given an azeotropic mixture A–B, the entrainer E should interact selectively with the original components and increase or decrease their relative volatility. Hereafter, we assume that A has a lower boiling temperature than B.

**2.1. Column Configuration and Operation.** Extractive distillation can be operated either in batch mode or in continuous mode. Because we consider a heavy entrainer (boiling temperature above those of both A and B), the entrainer stream is fed above the main feed in the continuous process configuration (Figure 1a) or above the boiler in the batch configuration (Figure 1b).

For continuous operation, the entrainer can be fed with the main feed (no extractive-section azeotrope distillation), above the main feed, or at the top of the column (no rectification section). This leads to three configurations for homogeneous continuous extractive distillation, which expands to seven for heterogeneous continuous extractive distillation according to Rodríguez-Donis et al.<sup>35</sup> We consider the classical configuration displayed in Figure 1a, with the entrainer fed above the main feed, giving rise to three sections, namely, rectifying, extractive, and stripping sections.

Extractive batch distillation is a semibatch process, as the main feed, F, is loaded initially into the boiler, whereas the entrainer is fed continuously at a higher tray. With a heavy entrainer, the batch column is a rectifier, with an extractive section and a rectifying section (Figure 1b), and the product is removed as distillate from the top. Steger et al.<sup>36</sup> summarized the configuration alternatives for batch extractive distillation columns, with the entrainer fed continuously into the boiler (no extractive section), at the top (no rectification section), or at an intermediate position (Figure 1b). The last alternative gives the best results, as the feasibility of extractive distillation

requires the intersection of an extractive composition profile with a rectifying composition profile.<sup>30,37</sup> Extractive batch distillation in a rectifier runs in four steps. First, under infinite reflux ratio ( $R_\infty$ ) and no entrainer feeding, heating starts, and the step proceeds until the azeotrope is obtained at the top (class 1.0-1a) or at the bottom (class 1.0-2).<sup>36,38–41</sup> Second, the entrainer is fed continuously so as to quickly substitute the azeotropic product by a high-purity compound. Third, the reflux (or reboil) ratio becomes finite, and a product is removed. The final step consists of classical distillation of the accumulated entrainer and the remaining original compound. Continuous operation consists of the third step of the batch operation.

**2.2. Extractive Distillation Feasibility Assessment.** The design of conventional and azeotropic distillation is related to thermodynamics, in particular, to the volatility of each compound and azeotrope. Furthermore, residue curve map analysis allows the feasibility to be assessed under infinite-reflux-ratio conditions and the ultimate products under direct or indirect split conditions to be identified.<sup>13</sup> However, distillation runs under finite-reflux-ratio conditions, and determining the achievable products and the location of the suitable feed composition region is more complicated because the composition profiles then depend on the reflux ratio.<sup>42–44</sup> That affects the range of concentration available to each section profile, because of the occurrence of pinch points that differ from the singular points of the residue curve map.<sup>45–48</sup>

The design of extractive distillation columns is further complicated by the occurrence of a middle extractive section, and the process often shows counterintuitive operating properties. The separation maximum and efficiency are not necessarily improved by increasing the reflux ratio,<sup>29</sup> and batch extractive distillation studies have further demonstrated the importance of selecting a suitable entrainer feed flow rate.<sup>40</sup>

From basic mass balance analysis, the feasibility of an extractive distillation under finite-reflux-ratio conditions requires that the global feed and top and bottom product compositions be collinear and that the top and bottom product composition points be connected to each other through the liquid composition profiles  $x_i$  in each section. Once a target product composition is set, the process feasibility depends on parameters such as the feed heat condition  $q$ , the feed stage location, the total number of stages, the column holdup, the vapor flow rate, the condenser cooling duty, and the boiler heat duty. However, the two parameters that are most important and that we consider remain the reflux ratio and the entrainer flow rate. Finding the ranges of the reflux ratio and entrainer flow rate that enable a feasible extractive distillation for a given

product purity is the main issue in extractive distillation. For the separation of a minimum-boiling azeotrope with a heavy entrainer, an estimation of the minimum amount of entrainer to be used is given by computing the solvent-free concentration diagram for the vapor concentration  $y_A^{noS}$  versus the liquid concentration  $x_A^{noS}$ . The minimum entrainer concentration is found when the azeotrope no longer exists in a plot of  $y_A^{noS}$  versus  $x_A^{noS}$ .<sup>15</sup>

**2.2.1. Thermodynamic Insight.** When using the popular feasibility rule that a heavy entrainer forming no new azeotrope is suitable to separate a minimum-boiling azeotrope, the corresponding A–B–E ternary diagram belongs to Serafimov's class 1.0-1a (21.6% occurrence). As Laroche et al.<sup>49,50</sup> showed for class 1.0-1a, knowledge of the residue curve map and the location of the univolatility curve  $\alpha_{AB} = 1$  can help assess which product is removed in the distillate when using a light, intermediate, or heavy entrainer. With a heavy entrainer, A (or B) can be distilled using a direct sequence if the univolatility curve intersects the A–E (B–E) edge. This helps explain the counterintuitive observation that, sometimes, the intermediate-boiling compound B within the A–B–E mixture is removed in the distillate.

The important separation of a maximum-boiling azeotrope with a heavy entrainer corresponds to class 1.0-2 (8.5% occurrence). It has not been studied in continuous operation but was studied in batch operation using composition profiles.<sup>51,52</sup>

The completion and extension of the thermodynamic insight to other mixture classes was published by Rodríguez-Donis et al.,<sup>30–34</sup> who combined knowledge of the thermodynamic properties of residue curve maps and of the univolatility and unidistribution curves location. They expressed a general feasibility criterion for extractive distillation under an infinite reflux ratio as follows: "homogeneous extractive distillation of an A–B mixture with entrainer E feeding is feasible if there exists a residue curve connecting E to A or B following a decreasing (a) or increasing (b) temperature direction inside the region where A or B is the most volatile (a) or the heaviest (b) component of the mixture". The volatility order is set by the univolatility curves.

Using illustrative examples covering all subcases, but exclusively operated in batch extractive distillation, those authors found that Serafimov's classes covering up to 53% of azeotropic mixtures were suited for extractive distillation: 0.0-1 (low-relative-volatility mixtures),<sup>31</sup> 1.0-1a, 1.0-1b, 1.0-2 (azeotropic mixtures with light, intermediate, or heavy entrainers forming no new azeotrope),<sup>30,32,33</sup> 2.0-1, 2.0-2a, 2.0-2b, and 2.0-2c (azeotropic mixtures with an entrainer forming one new azeotrope).<sup>34</sup> For all suitable classes, the general criterion under an infinite reflux ratio could explain the product to be recovered and the possible existence of limiting values for the entrainer flow rate for batch operation: a minimum value for class 1.0-1a, a maximum value for class 1.0-2, and so on. The behavior at finite reflux ratio could be deduced from the infinite-reflux-ratio behavior and properties of the residue curve maps, and some limits on the reflux ratio were found. However, precise determination of the limiting values of the reflux ratio or entrainer flow rate required other techniques, as summarized next.

**2.2.2. Intersection of Composition Profiles.** Initial studies extended methods developed for single-feed azeotropic distillation columns to double-feed columns for the analysis of extractive distillation processes by examining the composi-

tion profiles in each column section.<sup>53,54</sup> The finding of pinch points for each section profile allowed the limiting values of the operating parameters to be determined.

Some earlier works<sup>45,53</sup> relied on plate-by-plate calculations, leading to discrete profiles with segments numbers that matched the equilibrium number of trays in each section. A differential approach was proposed by Van Dongen and Doherty<sup>55</sup> and used by Lelkes et al.<sup>40,41</sup> for batch extractive distillation. In addition, a complete set of differential expressions for the composition profiles was published by Rodríguez-Donis et al.<sup>35</sup> for continuous heterogeneous extractive distillation; it also holds for homogeneous extractive distillation. The model is based on the following simplifying assumptions: (1) theoretical plates, (2) saturated liquid feed, (3) constant molar flow rates of liquid in the three sections of the column, (4) constant molar vapor flow rate throughout the column, and (5) incompressible fluid.

**Stripping section**

$$\frac{dx_i}{dh} = \frac{S}{S+1} \left[ \left( 1 + \frac{1}{S} \right) x_i - \frac{1}{S} x_W - y_i^* \right] \quad (1)$$

In eq 1,  $y_i^*$  is the concentration of compound  $i$  in the vapor in equilibrium with  $x_i$ ,  $y_i^*$  is computed by using a proper thermodynamic model, and  $S$  is the reboil ratio and is equal to  $V/W$ .

**Extractive section**

$$\begin{aligned} \frac{dx_i}{dh} = \frac{R+1}{R + \left( \frac{F_E}{F} \right) \left( \frac{F}{D} \right)} & \left\{ \left[ \frac{R}{R+1} + \frac{1}{R+1} \left( \frac{F_E}{F} \right) \left( \frac{F}{D} \right) \right] x_i \right. \\ & \left. + \frac{1}{R+1} x_D - \frac{1}{R+1} \left( \frac{F_E}{F} \right) \left( \frac{F}{D} \right) x_E - y_i^* \right\} \end{aligned} \quad (2)$$

In eq 2,  $R$  is the reflux ratio, which is equal to  $L_T/D$  (see Figure 1 for notation). A simple mass balance can show that this expression is equivalent to the one for batch distillation that was used by Rodríguez-Donis et al.<sup>30</sup> to validate their general feasibility criterion under infinite-reflux-ratio conditions for extractive distillation

$$\begin{aligned} \frac{dx_i}{dh} = \frac{R+1}{R + (R+1) \left( \frac{F_E}{V} \right)} & \left\{ \left[ \frac{R}{R+1} + \left( \frac{F_E}{V} \right) \right] x_i \right. \\ & \left. + \frac{1}{R+1} x_D - \left( \frac{F_E}{V} \right) x_E - y_i^* \right\} \end{aligned} \quad (3)$$

**Rectifying section**

$$\frac{dx_i}{dh} = \frac{R+1}{R} \left[ \left( \frac{R}{R+1} \right) x_i + \frac{1}{R+1} x_D - y_i^* \right] \quad (4)$$

In these equations, setting the reboil ratio  $S$  or the reflux ratio  $R$  as infinite and the entrainer feed flow rate  $F_E$  equal to 0 leads to the residue curve equation

$$\frac{dx_i}{dh} = x_i - y_i^* \quad (5)$$

The straightforward calculation method consists of selecting a column configuration and values for the reflux ratio and the entrainer flow rate. Assuming a direct (fixed  $x_D$ ) or indirect (fixed  $x_W$ ) split and a recovery rate, the other product is computed from the overall mass balance, as the main feed  $x_F$



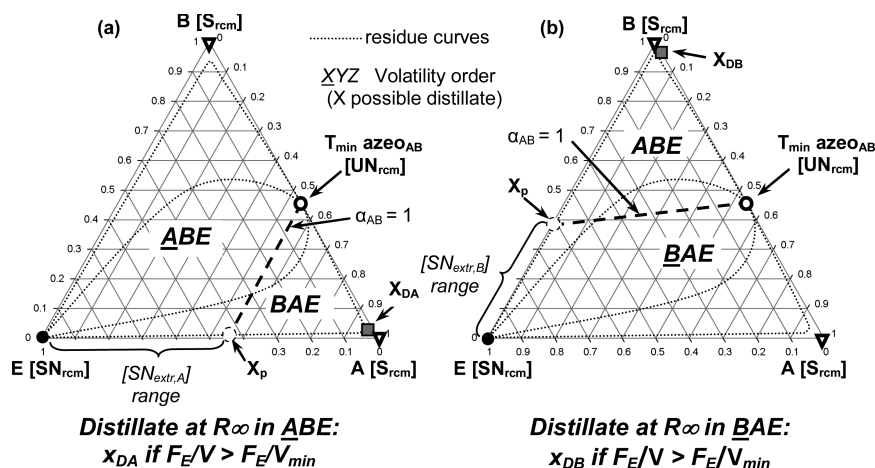


**Figure 2.** Thermodynamic features of class 1.0-1a mixtures with respect to batch extractive distillation: separation of a minimum-boiling azeotrope with a heavy entrainer.

and the entrainer feed  $x_E$  compositions and flow rates are known. The rectifying-liquid composition profile is computed top-down from the reflux ratio composition, which, here, in a homogeneous process, is equal to  $x_D$ . (See Rodríguez-Donis et al.<sup>35</sup> for a complete discussion of heterogeneous variants.) The stripping-liquid composition profile is computed bottom-up from  $x_W$ . The extractive distillation profile is computed from any composition belonging to either the rectifying or stripping composition profile, the choice of which is user-dependent. Limiting reflux ratio or entrainer flow rate values can then be found from the map analysis.

**2.2.3. Pinch-Point Analysis.** The search for limiting values of the reflux ratio and entrainer flow rate has been more systematized by the use of an algebraic criterion<sup>53</sup> or of mathematical approaches such as bifurcation theory,<sup>56</sup> interval arithmetics,<sup>37</sup> or the combined bifurcation–shortcut rectification body method.<sup>57</sup>

Extending its method for single-feed azeotropic distillations,<sup>45</sup> Levy et al.<sup>53</sup> proposed an algebraic trial-and-error tangent-pinch-point procedure for determining the minimum reflux ratio without the necessity of lengthy iteration schemes involving column profile calculations. The method consisted of finding the value of the reflux ratio that makes the feed pinch point, the saddle pinch point, and the controlling feed composition collinear but was restricted to ternary mixtures.

After studying the sequence of the extractive column with the entrainer regeneration column for the separation of the acetone–methanol azeotrope with water, belonging to class 1.0-1a,<sup>28</sup> Knapp and Doherty<sup>29</sup> used bifurcation theory to analyze class 1.0-1a behavior and related the feasibility of the extractive process to the appearance of saddle-node bifurcation points and branching points. Feasible processes required that a ternary saddle originating from a pure component existed, whereas the appearance of a ternary unstable node on the pinch branch originating at the azeotrope led to an unfeasible separation. They also proposed some heuristics to set the operating values of  $R$  and  $F_E$ , once their minimum values were known. They also published more general diagrams, originating from bifurcation theory, without providing any illustrative examples.

Frits et al.<sup>37</sup> used an interval-arithmetic-based branch-and-bound optimizer to find limiting flows based on the existence and location of singular points and separatrices in profile maps.

They applied it to the acetone–methanol–water class 1.0-1a mixture on batch extractive distillation. In agreement with the findings of Knapp and Doherty for continuous processes, the process was found to be feasible under infinite-reflux-ratio conditions above a minimum entrainer flow rate that corresponded to the merging of a stable pinch point originating from the azeotrope with a saddle point originating from a pure component. Finite-reflux-ratio analysis showed that the pinch points moved inside the composition triangle and brought unfeasible regions, as described later.

Brüggemann and Marquardt<sup>57</sup> exploited a fully automated shortcut design procedure to determine the limit values of the reflux ratio and entrainer flow rate. The method is based on the approximation of all column profiles by the so-called rectification body method (RBM), which is constructed from nonlinear analysis of the pinches of each section.<sup>47</sup> Similarly to Knapp and Doherty,<sup>29</sup> they also set some operating constraints to determine the quasi-optimal values once the minimum values of  $R$  and  $F_E$  were known. Several ternary mixtures were used for illustration, all of them belonging to class 1.0-1a, but a quaternary mixture with two azeotropes and an entrainer forming no new azeotrope was also shown. Kossack et al.<sup>58</sup> then used the RBM as a second screening criterion for evaluating candidates for the extractive distillation entrainer. Fast and efficient, the method encounters some difficulties when the profiles are highly curved because each rectification body has straight boundaries.<sup>59</sup>

Finally, one should notice the recent publication of a noniterative method for finding the possible splits of azeotropic distillation at finite reflux ratio based on the identification of the common terminal points of pinch branches in each column section.<sup>60,61</sup> Its extension to extractive distillation is in preparation.

Although these methods are invaluable in obtaining accurate limiting values, they have mostly been illustrated for mixtures belonging to class 1.0-1a, namely, the separation of minimum-(maximum-) boiling azeotrope with heavy (light) entrainers.

### 3. FEASIBILITY STUDY METHODOLOGY

Our methodology aims at extending thermodynamic insights for batch extractive distillation to continuous distillation. Compared to the batch column configuration, the continuous column configuration has an additional stripping section (see

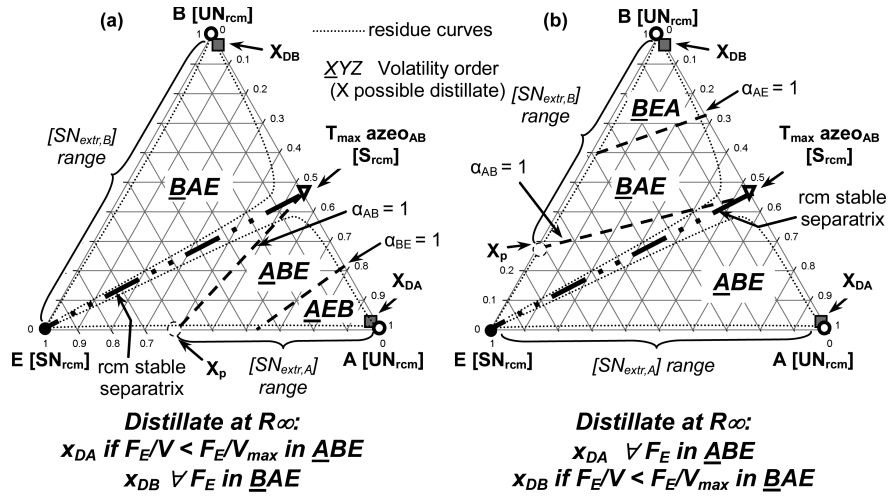


**Figure 3.** Thermodynamic features of class 1.0-2 mixtures with respect to batch extractive distillation: separation of a maximum-boiling azeotrope with a heavy entrainer.

Figure 1). The key parameters remain the reflux ratio  $R$  and the entrainer/feed flow rate ratio  $F_E/F$  for continuous operating mode or  $F_E/V$  for batch mode, where  $V$  is the vapor flow rate going up from the boiler. The methodology proceeds in three steps: Step 1 assumes that the possible products identified from the thermodynamic insight for batch extractive distillation are valid for the continuous process. It also transforms the limiting values of the entrainer/feed flow rate ratio,  $F_E/V$ , found for the batch process into a entrainer/feed flow rate ratio,  $F_E/F$ , for the continuous process. Step 2 aims at finding the feasible ranges of the operating parameters reflux ratio and entrainer/feed flow rate ratio and comparing the batch and extractive processes. In step 3, rigorous simulation is used to confirm step 2.

**3.1. Step 1. Thermodynamic Feasibility Criterion for Ternary Diagram Classes 1.0-1a and 1.0-2.** **3.1.1. Product and Limiting Operating Parameter Value for Batch Extractive Distillation Process.** We used the general feasibility criterion published by Rodríguez-Donis et al.<sup>30</sup> and validated for batch extractive distillation. It suggests the expected product and the possible occurrence of limiting values for the reflux ratio and the entrainer flow rate ratio  $F_E/V$ .

Figure 2 displays the essential features of class 1.0-1a, corresponding to the separation by extractive distillation of a minimum-boiling azeotropic mixture A–B with a heavy entrainer E.

The occurrence of Serafimov's class 1.0-1a in the literature amounts to 21.6%.<sup>62</sup> With a heavy entrainer, the light original component A and the heavy original component B are both saddle points on the residue curve map (rcm) and form a minimum-boiling azeotrope,  $T_{\min} \text{ azeo}_{AB}$ , which is a rcm unstable node. The univolatility curve  $\alpha_{AB} = 1$  switches the volatility order of the concerned compounds, and the volatility orders are ABE or BAE (see Figure 2) depending on the side.<sup>11</sup> Two subcases arise. In Figure 2a, the  $\alpha_{AB} = 1$  curve intersects binary side A–E at the so-called point  $x_p$ . Then, A is the expected product in the distillate because it is the most volatile in the region where it is related to E by a residue curve of decreasing temperature from E to A. This matches the general feasibility criterion under an infinite reflux ratio for batch distillation.<sup>30</sup> In Figure 2b, the  $\alpha_{AB} = 1$  curve intersects binary side B–E, and B is then the expected product.

Analysis of the composition profile maps and pinch points under an infinite reflux ratio have shown that the extractive distillation process is feasible only if the entrainer flow rate ratio  $F_E/V$  is greater than a minimum value  $(F_E/V)_{\min}$ .<sup>29,30,37</sup>  $F_E/V$  is the governing parameter of the extractive composition profile in eq 3 that holds for batch distillation. Below  $(F_E/V)_{\min}$ , the terminal point of the extractive section profiles,  $SN_{\text{extr}}$  lies on the univolatility curve. Above  $(F_E/V)_{\min}$ ,  $SN_{\text{extr}}$  leaves the univolatility curve to lie near the  $[x_p, E]$  segment. Then, the extractive profile can cross a rectifying profile, which is approximated by a residue curve under infinite reflux ratio and which reaches the vicinity of the product, namely, A.

Figure 3 displays the essential features of class 1.0-2 corresponding to the separation by extractive distillation of a maximum-boiling azeotropic mixture A–B with a heavy entrainer E:

The occurrence of Serafimov's class 1.0-2 in the literature is 8.5%.<sup>62</sup> The class 1.0-2 diagram displays a rcm stable separatrix that divides the composition space into two distillation regions. With a heavy entrainer, it connects the stable node E to the saddle-point maximum-boiling azeotrope  $T_{\max} \text{ azeo}_{AB}$ . Both components A and B are rcm unstable nodes. The size of the volatility order regions BAE (and eventually BEA) and ABE (and eventually AEB) depends on the location of the  $\alpha_{AB} = 1$  univolatility curve (Figure 3). The other univolatility curve ( $\alpha_{BE} = 1$  in Figure 3a or  $\alpha_{AE} = 1$  in Figure 3b) might exist,<sup>11</sup> but it does not affect the findings of the extractive distillation feasibility and product.<sup>30</sup> Both A and B are connected by a residue curve of decreasing temperature to E, which nears the triangle edge in the ternary diagram. Therefore, both A and B can be distillate products, depending on the location of the global feed composition  $x_F + x_{FE}$ , either in  $\underline{BAE}$  and  $\underline{BEA}$  (B product) or in  $\underline{ABE}$  and  $\underline{AEB}$  (A product). To add more explanation, recall that, at an infinitesimal entrainer flow rate, the rcm singular points become the singular points of the extractive profile map with an opposite stability for the heavy entrainer case.<sup>29,37</sup> When the entrainer flow rate is increased for class 1.0-2, the singular points of the extractive profile,  $SN_{\text{extr},A}$  and  $SN_{\text{extr},B}$ , originating from A and B, respectively, move toward the entrainer vertex.<sup>30</sup> In Figure 3a,  $SN_{\text{extr},B}$  can go up to E and there is no limiting flow rate. But  $SN_{\text{extr},A}$  disappears at point  $x_p$  when it merges with the saddle extractive,  $S_{\text{ext}}$ .

originating at the  $T_{\max}$  aze<sub>AB</sub>. Thus, there is a maximum entrainer/feed flow rate ratio  $(F_E/V)_{\max}$  to obtain A as a product by extractive distillation. The opposite occurs in Figure 3b. This behavior is directly related to the volatility order regions, which explains how the general criterion was established. The exact value of  $(F_E/V)_{\max}$  can be readily calculated.

We expect the general feasibility criterion for batch mode to hold for the intersection of the extractive and rectifying section of the continuous distillation column (Figure 1a), as those already exist in batch distillation column (Figure 1b).

**3.1.2. Product and Limiting Operating Value for Continuous Extractive Distillation Process.** Knowledge of the existence of limiting values for the entrainer flow rate ratio in batch mode, namely, a minimum value for  $F_E/V$  for class 1.0-1a and a maximum for class 1.0-2, is transformed into a limiting entrainer/feed ratio  $F_E/F$  for continuous mode by means of the equation

$$\left(\frac{F_E}{F}\right) = (R + 1) \left(\frac{F_E}{V}\right) \left(\frac{D}{F}\right) \quad (6)$$

This equation shows that the limiting value for  $F_E$  depends on  $R$  and  $D$ . As the distillate composition  $x_D$  is chosen to compute the composition profiles, setting a distillate recovery enables the computation of  $D$  from the mass balance, once the main and entrainer feed compositions and flow rates are known. Table 1 summarizes these data for all mixtures.

**3.2. Step 2. Calculation of the Feasible Ranges of the Reflux Ratio and Entrainer/Feed Flow Rate Ratio.** The extractive distillation feasibility is determined by computing continuous composition profiles maps for all three sections from eqs 1 (rectifying section), 2 (extractive section), and 4 (stripping section) and visually checking their intersection. The feasibility of the batch extractive distillation process requires that the extractive and rectifying section profiles intersect. The continuous process requires the intersection of the stripping and extractive profiles as well.

Product purity and recovery are fixed (see Table 1), enabling all of the needed parameter values to be determined from the mass balances, once the entrainer and feed stream compositions and flow rates are given.

The results are displayed as plots of the entrainer/feed flow rate  $F_E/F$  versus the reflux ratio  $R$  for continuous mode and of  $F_E/V$  versus  $R$  for batch mode, where the feasible parameter ranges for the batch and continuous processes are sketched. Note that the obtained results are dependent on the target purity and recovery and on the choice of thermodynamic model used to compute  $y_i^*$ . This last point should first be validated carefully against experimental data for any industrial use of the methodology.

**3.3. Step 3. Rigorous Simulation.** Rigorous simulation with a MESH (mass, equilibrium, summation, and heat) equilibrium distillation column model using either ProSimPlus 3.1<sup>63</sup> or Aspen Plus 11.1<sup>64</sup> software is run to check the feasibility predictions of step 2. Considering fixed values of the reflux ratio and entrainer/feed flow rate ratio and composition, these simulations provide the exact distillate and bottom compositions, along with the stage compositions, flows of liquid and vapor, and temperatures. These simulations consider energy balances, although they are not expected to play a significant part in feasibility.

**Table 1. Operating Parameters<sup>a</sup> for All Case Studies**

product		A	B	E		
Class 1.0-1a Case a: A (Acetone)–B (Heptane) + E (Toluene)						
A (acetone)	$x_F$	0.9	0.1	0	$D$	0.9
	$x_E$	0	0	1	$W$	10.1
	$x_D$	0.98	0.01	0.01	$F$	1
	$x_W$	0.0018	0.0090	0.9892	$F_E/F$	10
	$\eta_b$	0.98	0	0	$R$	20
	$x_F + x_E$	0.0818	0.0092	0.9090	$F_E/V$	0.53
Class 1.0-1a Case b: A (Acetone)–B (Methanol) + E (Chlorobenzene)						
B (methanol)	$x_F$	0.1	0.9	0	$D$	0.9
	$x_E$	0	0	1	$W$	10.1
	$x_D$	0.01	0.98	0.01	$F$	1
	$x_W$	0.0090	0.0018	0.9892	$F_E/F$	10
	$\eta_b$	0	0.98	0	$R$	10
	$x_F + x_E$	0.0092	0.0818	0.9090	$F_E/V$	1.01
Class 1.0-2 Case a: A (Chloroform)–B (Vinyl Acetate) + E (Butyl Acetate)						
A (chloroform)	$x_F$	0.9	0.1	0	$D$	0.8909
	$x_E$	0	0	1	$W$	10.11
	$x_D$	0.990	0.005	0.005	$F$	1
	$x_W$	0.0018	0.0094	0.9888	$F_E/F$	10
	$\eta_b$	0.98	0	0	$R$	15
	$x_F + x_E$	0.0818	0.0091	0.9091	$F_E/V$	0.7015
B (vinyl acetate)	$x_F$	0.1	0.9	0	$D$	0.8909
	$x_E$	0	0	1	$W$	10.11
	$x_D$	0.005	0.990	0.005	$F$	1
	$x_W$	0.0094	0.0018	0.9888	$F_E/F$	10
	$\eta_b$	0	0.98	0	$R$	15
	$x_F + x_E$	0.0091	0.0818	0.9091	$F_E/V$	0.7015
Class 1.0-2 Case b: A (Acetone)–B (Chloroform) + E (Benzene)						
A (acetone)	$x_F$	0.9	0.1	0	$D$	0.9
	$x_E$	0.1	0	0.9	$W$	10.1
	$x_D$	0.98	0.01	0.01	$F$	1
	$x_W$	0.1008	0.0090	0.8902	$F_E/F$	10
	$\eta_b$	0.98	0	0	$R$	15
	$x_F + x_E$	0.1728	0.0091	0.8181	$F_E/V$	0.694
B (chloroform)	$x_F$	0.1	0.9	0	$D$	0.9
	$x_E$	0	0.1	0.9	$W$	10.1
	$x_D$	0.01	0.98	0.01	$F$	1
	$x_W$	0.0090	0.1008	0.8902	$F_E/F$	10
	$\eta_b$	0	0.98	0	$R$	15
	$x_F + x_E$	0.0091	0.1728	0.8181	$F_E/V$	0.694

<sup>a</sup> $x_F$ , mole fraction in the main feed;  $x_E$ , mole fraction in the entrainer feed;  $x_D$ , top composition;  $x_W$ , bottom composition;  $\eta_b$ , product recovery;  $x_F + x_E$ , global mole fraction in the feed;  $D$ , distillate flow rate;  $W$ , bottom flow rate;  $F$ , feed flow rate;  $F_E/F$ , continuous entrainer/feed ratio;  $R$ , reflux ratio;  $F_E/V$ , batch entrainer/feed ratio.

The step 3 simulation is used to confirm step 2 and is not aimed at optimizing the separation, in particular, with respect to the reflux ratio, energy demand, entrainer/feed flow rate, or number of trays in each section. Such an optimization is outside our scope and should be done for a column sequence with both extractive distillation and entrainer regeneration columns.<sup>65,66</sup> The number of trays in the extractive section is set at a proper value so that the terminal point of the composition profile of the extractive section is near the extractive section stable node. For all illustrated mixtures, the modified (Dortmund) UNIFAC thermodynamic model (1993) is used. Table 2 lists the specifications of the extractive distillation column.

**Table 2. Column Operating Specifications for Rigorous Simulation**

parameter	class 1.0.1-a		class 1.0.2
	case a	case b	cases a and b
number of trays, $N$	22	22	40
entrainer tray, $N_{FE}$	7	7	5
feed tray, $N_F$	14	14	15
$x_F$ (A, B, E)	(0.9, 0.1, 0.0)	(0.1, 0.9, 0.0)	(0.1, 0.9, 0.0)
$x_E$ (A, B, E)	(0.0, 0.0, 1.0)	(0.0, 0.0, 1.0)	(0.0, 0.0, 1.0)

## 4. RESULTS

**4.1. Separation of Minimum-Boiling-Temperature Azeotropes with Heavy Entrainers (Class 1.0-1a).** In this section, we consider the separation of a minimum-boiling azeotrope A–B with a heavy entrainer E. The ternary mixture belongs to Serafimov's class 1.0-1a and is split into two cases in which the  $\alpha_{AB} = 1$  curve intersects binary side A–E or B–E (Figure 2).

**4.1.1. Class 1.0-1a Case a:  $\alpha_{AB} = 1$  Curve Reaches Binary Side A–E.** Figure 4a displays the residue curve map (rcm) under  $R_\infty$  for the minimum-boiling azeotropes acetone (A, 56.3 °C)–heptane (B, 98.4 °C) ( $x_{azeo,A} = 0.93$  at 55.8 °C) with heavy entrainer toluene (E, 110.6 °C). The  $\alpha_{AB} = 1$  curve intersects binary side A–E.

An infinitely small increase in entrainer flow rate,  $F_E/V = 0.01$ , highlights the features of the extractive profile map (Figure 4b): The stability of the singular points of the extractive profile is now opposite that of the rcm one.<sup>29</sup> The profile shapes are close to rcm ones. As  $F_E$  increases, the extractive stable node  $SN_{extr}$  moves along the univolatility curve until it merges near the A–E edge with the extractive saddle

originating in A, for  $(F_E/V)_{min}$ , estimated at 0.12 for  $R_\infty$ . Above  $(F_E/V)_{min}$  (Figure 4c),  $SN_{extr,A}$  lies near the A–E edge, and the extractive process becomes feasible. A is then the unique possible distillate cut, because all of the extractive composition profiles reach  $SN_{extr,A}$  where they intersect a rectifying section profile, namely, a residue curve as  $R$  is infinite, nearing A. At the same time, the saddle  $S_{extr,B}$  originating from B moves along the B–E edge toward E, but the whole composition triangle allows the process to be feasible. If the reflux ratio becomes finite (Figure 4d),  $S_{extr,B}$  and  $UN_{extr}$  move inside the triangle, giving rise to an unstable extractive separatrix, which, in turn, defines an unfeasible composition region near the B–E edge: The extractive profile no longer reaches  $SN_{extr,A}$  and A is not the distillate product. At very low reflux ratio, the unfeasible region overcomes  $SN_{extr,A}$  and the process is no longer feasible.

To extend this insight from batch mode to continuous mode, we follow the three-step methodology described in section 3. In step 1, eq 6 translates the occurrence of a minimum value for  $F_E/V$  to obtain a feasible batch process into a minimum value for  $F_E/F$  that depends on  $R$ . For the batch column configuration (Figure 1b), the minimum value was related to the need to have an extractive section profile that intersects a rectifying profile nearing the product vertex. For the continuous configuration (Figure 1a), the feasibility also requires that the extractive section profile intersect the stripping section profile to reach the bottom product  $x_W$ , computed from mass balances (Table 1).

That is systematically checked in step 2 by computing the section profiles for various pairs of values of  $F_E/F$  and  $R$  and checking whether they intersect each other. The feasible ranges of the operating parameters for the batch and continuous

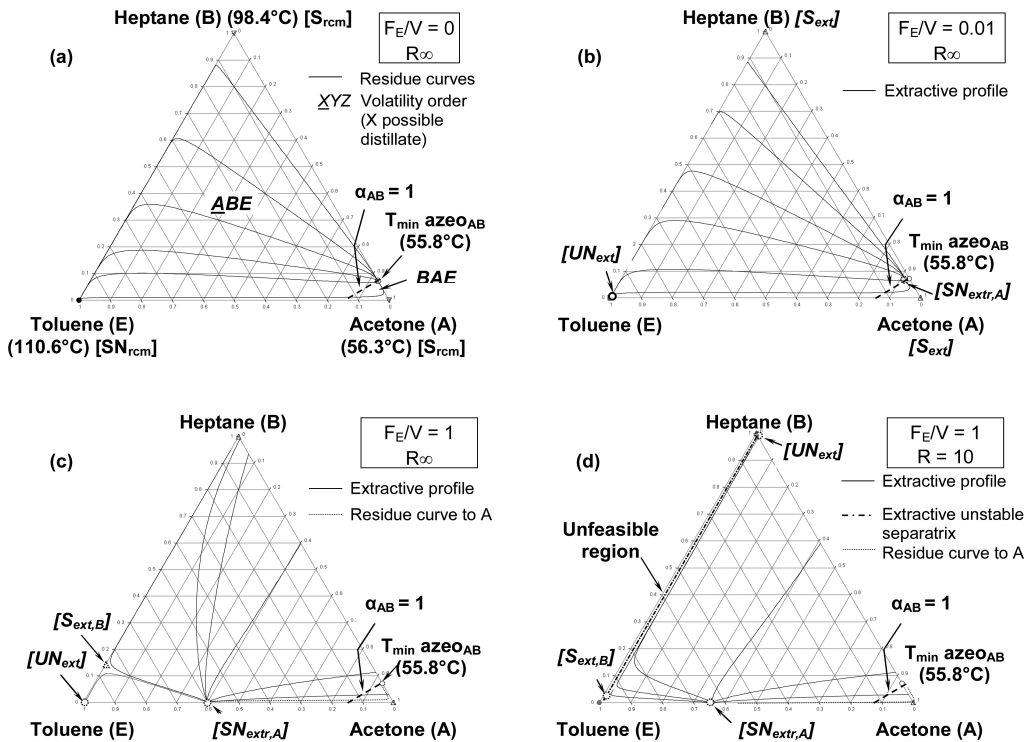


**Figure 4.** Separation of acetone–heptane using toluene: (a) class 1.0-1a residue curve map (rcm) and batch extractive profile map; (b)  $F_E/V = 0.01$ ,  $R_\infty$ ; (c)  $F_E/V = 1$ ,  $R_\infty$ ; and (d)  $F_E/V = 1$ ,  $R = 10$ .

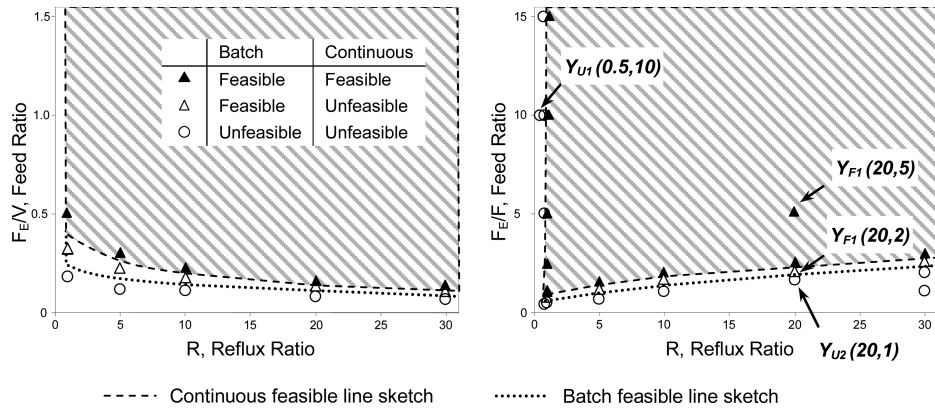


**Figure 5.** Feasibility of batch and continuous extractive distillation of acetone–heptane with toluene (class 1.0-1a). Feed ratio as a function of the reflux ratio expressed as a (a) batch or (b) continuous variable.

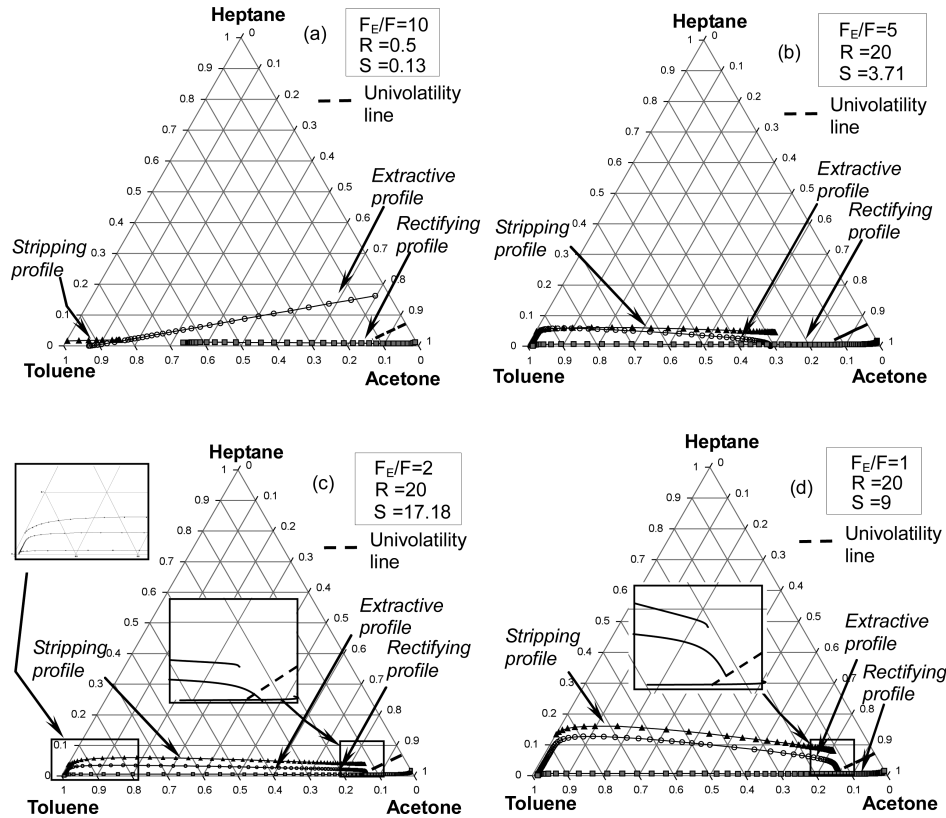


**Figure 6.** Rectifying, extractive, and stripping compositions for four operating parameter points taken from Figure 5: (a) point  $Y_{U1}$ , (b) point  $Y_{F1}$ , (c) point  $Y_{U2}$ , and (d) point  $Y_{U3}$ .

processes to obtain A as the product with a purity of  $x_D$  and a recovery of  $\eta_b$  are displayed in terms of the entrainer/feed flow rate ratio  $F_E/V$  versus the reflux ratio  $R$  (Figure 5a) and  $F_E/F$  versus  $R$  (Figure 5b), respectively. Both graphs display the exact same results and use the same parameters (Table 1). The shape of the feasible region is different depending on the y-axis variable used,  $F_E/V$  or  $F_E/F$ , because, according to eq 6, when  $F_E/V$  is fixed,  $F_E/F$  is not directly proportional to  $R + 1$  but also to  $D/F$ .

One notices that the range of feasible reflux ratios to obtain the desired product purity increases as the entrainer/feed flow rate ratio. In addition, the feasible regions of both the batch and

continuous processes are bounded by a minimum value as predicted by step 1. A key result is that the minimum value is higher for the continuous process when the same purity is targeted. At  $R = 20$ , the batch process is feasible for  $F_E/V = 0.12$  (equivalent to  $F_E/F = 2.0$ ), whereas the continuous process is feasible above  $F_E/F = 2.5$  (equivalent to  $F_E/V = 0.15$ ).

Figure 6 displays the composition profiles computed for all three sections from eqs 1, 2, and 4 at four operating parameter points taken from Figure 5b. For  $Y_{U1}$  ( $R = 0.5$ ,  $F_E/F = 10$ ), the process is unfeasible for both batch and continuous modes because the rectifying profile falls short of intersecting the extractive section profile. The extractive section profile ends on

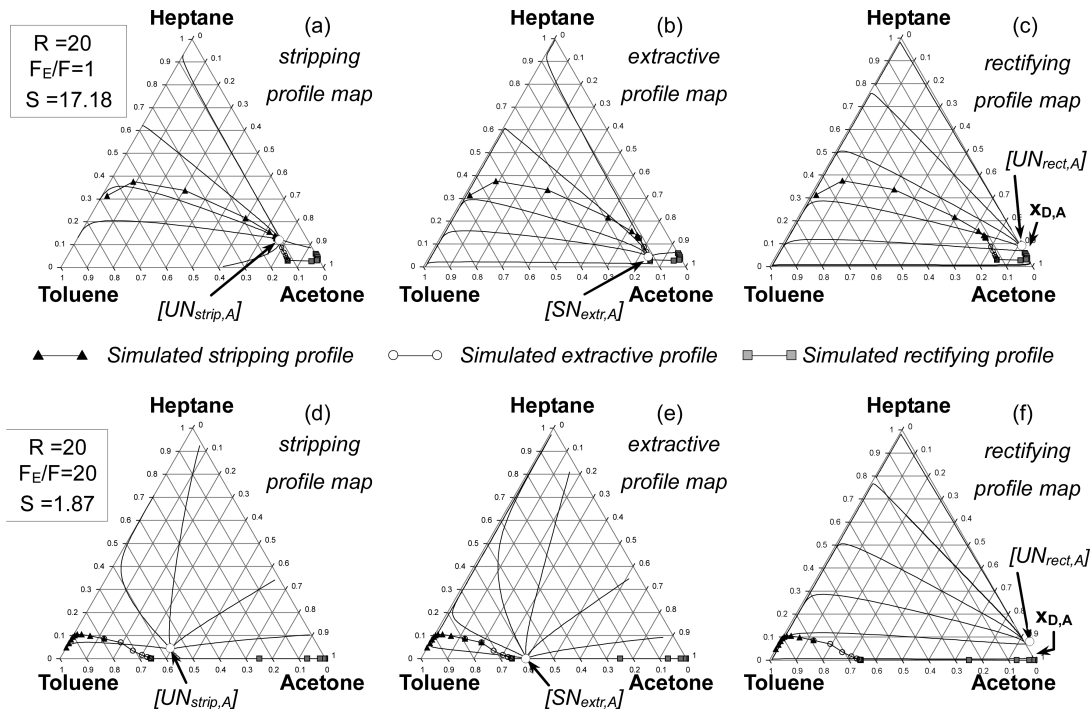


Figure 7. Rigorous simulation result to recover acetone at  $F_E/F = 1$ ,  $R = 20$  and  $F_E/F = 20$ ,  $R = 20$ , compared with calculated profiles: (a,d) stripping section, (b,e) extractive section, and (c,f) rectifying section.

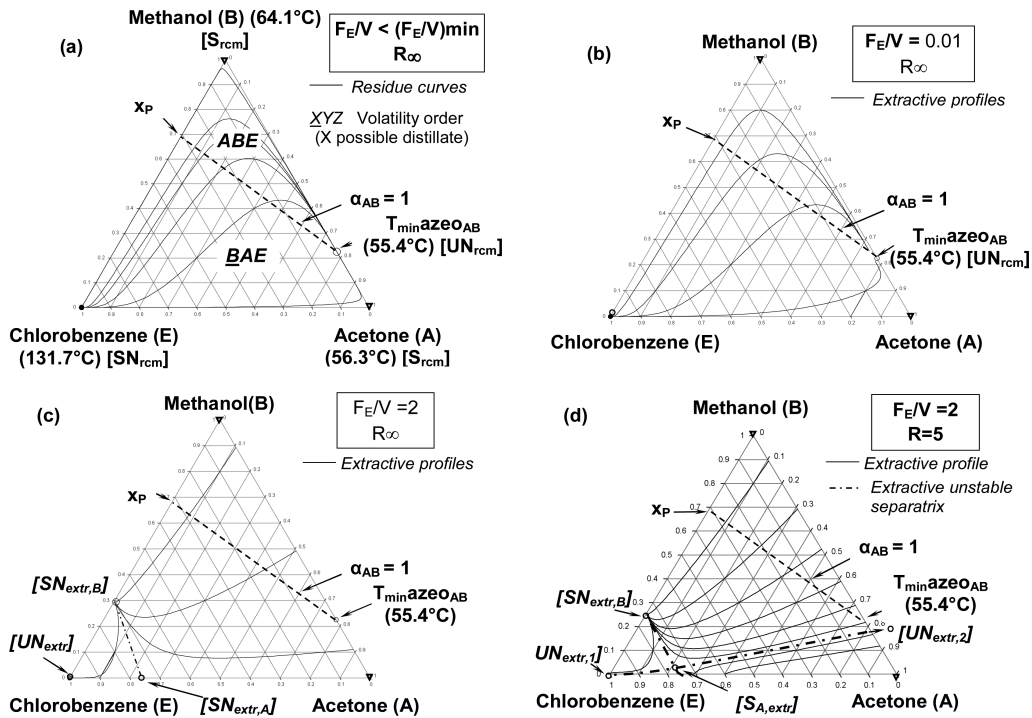
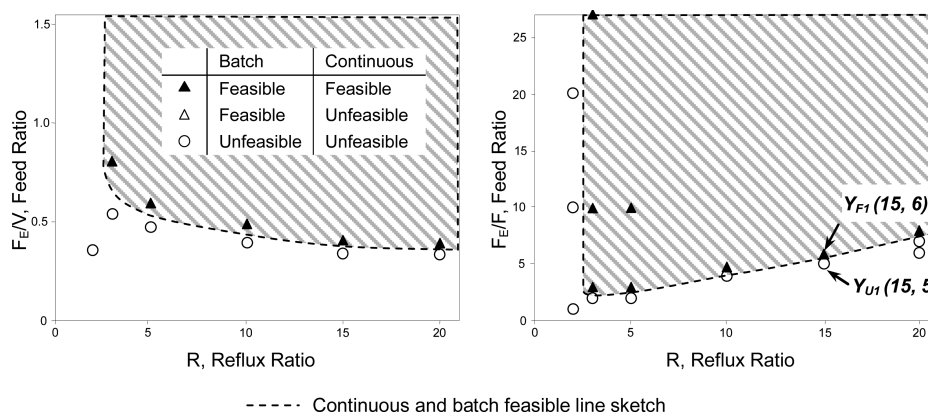


Figure 8. Separation of acetone–methanol using chlorobenzene: (a) class 1.0-1a residue curve map (rcm) and batch extractive profile map; (b)  $F_E/V = 0.01$ ,  $R_\infty$ ; (c)  $F_E/V = 2$ ,  $R_\infty$ ; and (d)  $F_E/V = 2$ ,  $R = 5$ .

a stable node  $SN_{extr}$  that is shifted toward vertex E as  $F_E/F$  increases (Figure 6a). For  $Y_{F1}$  ( $R = 20$ ,  $F_E/F = 5$ ), the process is feasible for both processes, as all section profiles intersect and the specified purity of 0.98 is reached (Figure 6b). For  $Y_{U2}$  ( $R = 20$ ,  $F_E/F = 2$ ), the continuous process is unfeasible because

there is no intersection between the profiles of the extractive and stripping sections, but the batch process feasible because the extractive and rectifying profiles intersect (Figure 6c). For  $Y_{U3}$  ( $R = 20$ ,  $F_E/F = 1$ ), no process is feasible, as none of the section profiles intersect each other (Figure 6d). The main





**Figure 9.** Feasibility of batch and continuous extractive distillation of acetone–methanol with chlorobenzene (class 1.0-1a). Feed ratio as a function of the reflux ratio to recover 98 mol % methanol (B) expressed as a (a) batch or (b) expressed in continuous variable.

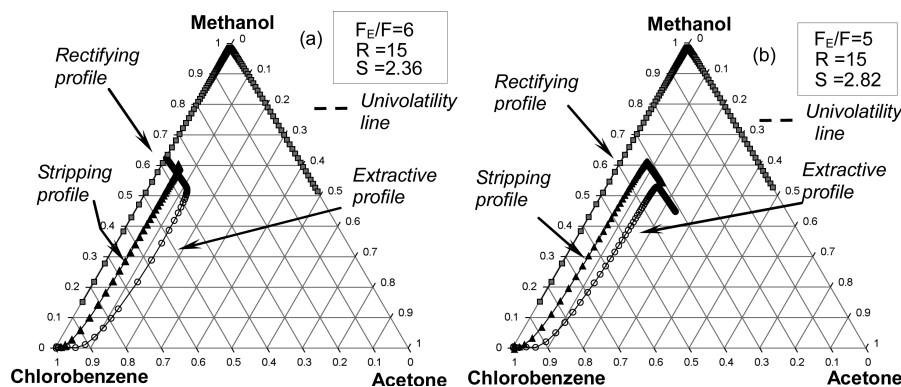


**Figure 10.** Rectifying, extractive, and stripping compositions for two operating parameter points taken from Figure 9: (a) point  $Y_{F1}$  and (b) point  $Y_{U1}$ .

result is that the feasible range of the continuous process is smaller than that of the batch process because the additional stripping profile in the continuous process must intersect the extractive profile to make the separation feasible.

Applying step 3 for further confirmation of these results, a rigorous simulation was carried out with Aspen Plus for an extractive column with the specifications listed in Table 2. The rigorous profiles are compared in Figure 7 to the approximate composition profile maps computed from eqs 1, 2, and 4, for a 98 mol % recovery and 98% purity in the distillate.

At  $F_E/F = 1$ , as predicted from Figure 6d, the rigorous simulation does not allow the recovery of 98 mol % acetone in the distillate; a value of 94.68 mol % is obtained instead. At such a low feed ratio, the  $F_E/V$  and  $F_E/F$  values are lower than that the minimum values for batch and continuous processes, respectively (Figure 5). The extractive stable node  $SN_{extr,A}$  lies on the univolatility curve (Figure 7c) and intersects a rectifying profile that cannot reach the targeted product purity (Figure 7e). Furthermore, the number of trays in the rectifying section is too large, forcing the composition to turn away from the acetone vertex toward the azeotrope. At  $F_E/F = 20$ , well within the feasible region in Figure 5,  $SN_{extr,A}$  lies near the A–E edge. The rigorous column distillate purity reaches 99.65%, above the target purity. Otherwise, the rigorous and approximate profiles shapes agree well with each other but not strictly because the rigorous profiles were computed using a fixed number of trays in each section whereas the differential equations for the

approximate profile are not dependent of the number of trays but can be related to an infinite number of trays.

**4.1.2. Class 1.0-1a Case b:  $\alpha_{AB} = 1$  Curve Reaches Binary Side B–E.** Figure 8 shows the residue curve map of the acetone (A, 56.3 °C)–methanol (B, 64.1 °C) ( $x_{azeo,A} = 0.78$  at 55.4 °C) with heavy entrainer chlorobenzene (E, 131.7 °C). The  $\alpha_{AB} = 1$  curve intersects binary side B–E. As detailed in Rodríguez-Donis et al.,<sup>30</sup> the expected behavior for batch extractive distillation is strictly identical to the previous case, except that B, the intermediate-boiling compound of the mixture, is now the distillate instead of compound A.

The extractive profile maps are also displayed under an infinite reflux ratio for  $F_E/V = 0.01 < (F_E/V)_{min}$  and  $F_E/V = 2 > (F_E/V)_{min}$ , with  $(F_E/V)_{min} \approx 0.4$ . As in class 1.0-1a case a, all extractive composition profiles end at  $SN_{B,extr}$  close to the B–E edge for  $F_E/V > (F_E/V)_{min}$ , making the batch process feasible. Under finite-reflux-ratio conditions (Figure 8d,  $F_E/V$ ,  $R = 5$ ), the saddle point  $S_{A,extr}$  moves inside the triangle and drags along an extractive unstable boundary with other unstable extractive nodes. This generates an unfeasible composition region that grows in size as the reflux ratio decreases, where the extractive composition profile reaches  $SN_{extr,A}$  instead of  $SN_{extr,B}$ .

Figure 9 displays the feasible range of operating conditions as feed ratio versus reflux ratio to recover 98 mol % methanol (B) as the univolatility line  $\alpha_{AB} = 1$  intersects binary side B–E. Its shape is similar to the Figure 5 case for the recovery of acetone (A) where the univolatility line  $\alpha_{AB} = 1$  intersects binary side

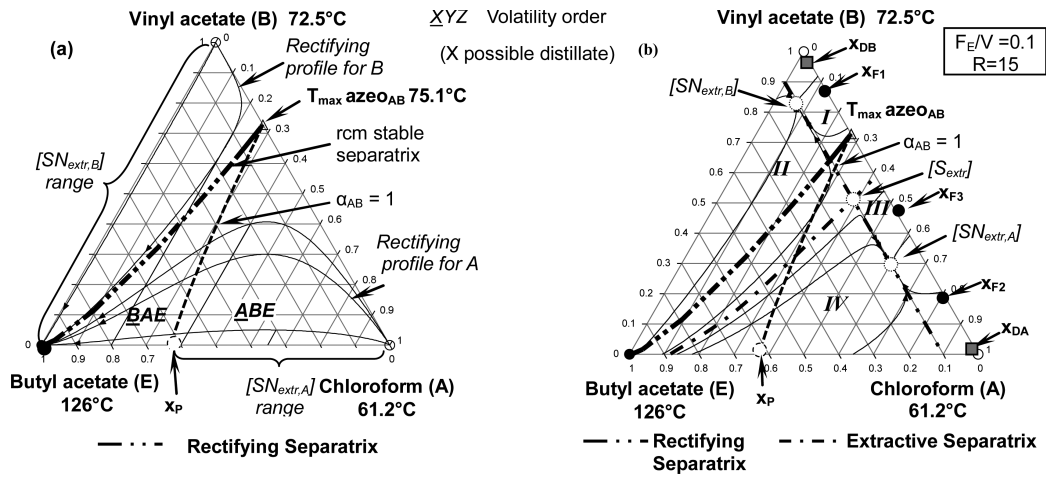


Figure 11. Separation of chloroform–vinyl acetate using butyl acetate: (a) class 1.0-2 residue curve map (rcm) and batch extractive profile map; (b)  $F_E/V = 0.1 < (F_E/V)_{\max}$   $R = 15$ .

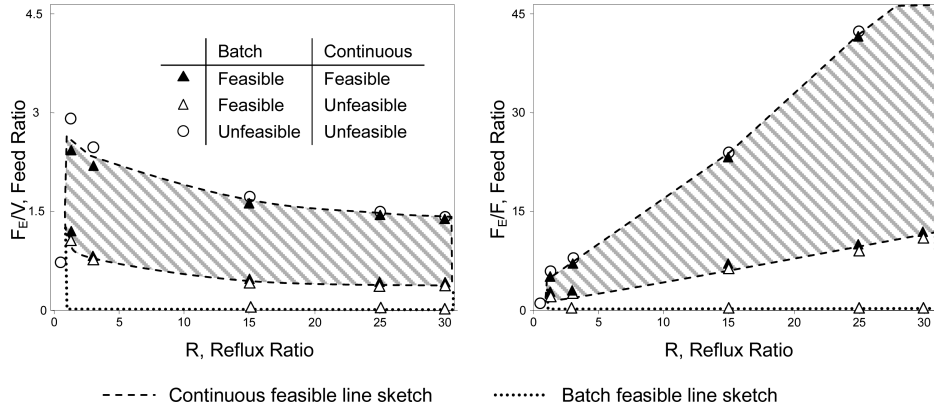


Figure 12. Feasibility of batch and continuous extractive distillation of chloroform–vinyl acetate with butyl acetate (class 1.0-2). Feed ratio as a function of the reflux ratio to recover 98 mol % chloroform (A) expressed as a (a) batch or (b) continuous variable.

A–E. However, for this mixture, the region for the batch process is not larger than that for the continuous process.

This can be explained from the composition profiles (Figure 10). For  $Y_{F1}$  ( $R = 15$ ,  $F_E/V = 6$ ), the process is feasible for both the batch and continuous processes, but it is not feasible for  $Y_{U1}$  ( $R = 15$ ,  $F_E/V = 5$ ), as the extractive and stripping profiles move in opposite directions (Figure 9b). Unlike the previous class 1.0-1a mixture, the feasible ranges of the batch and continuous processes are identical because the stripping section is located between the rectifying and extractive sections. Once the extractive profile no longer crosses the rectifying profile, it also does not cross the stripping profile.

**4.2. Separation of Maximum-Boiling Azeotropes with Heavy Entrainers (Class 1.0-2).** In this section, we consider the separation of a maximum-boiling azeotrope with a heavy entrainer. The ternary mixture belongs to Serafimov's class 1.0-2 and is split into two cases in which the  $\alpha_{AB} = 1$  curve intersects binary side A–E or B–E (Figure 3).

**4.2.1. Class 1.0-2 Case a:  $\alpha_{AB} = 1$  Curve Reaches Binary Side A–E.** Separation of the maximum-boiling azeotrope chloroform (A, 61.2 °C)–vinyl acetate (B, 72.5 °C) ( $x_{\text{azeo},A} = 0.28$  at 75.1 °C) with heavy entrainer butyl acetate (E, 126 °C) illustrates the case in which the  $\alpha_{AB} = 1$  curve reaches the A–E side (Figure 11). According to the general feasibility

criterion for extractive distillation under an infinite reflux ratio,<sup>30</sup> both chloroform (A) and vinyl acetate (B) can be recovered as distillate, depending on the global feed composition.

As the ranges of  $SN_{\text{extr},A}$  and  $SN_{\text{extr},B}$  show (Figure 11a), there exists a maximum value  $(F_E/V)_{\max,A,R,\infty}$  for recovering component A but no entrainer limit restriction to recover component B at infinite reflux ratio.<sup>30</sup> At finite reflux ratio and for  $(F_E/V) < (F_E/V)_{\max,A}$ , extractive separatrices appear, but they still allow the recovery of either A or B, depending on the global feed composition. Pure A can be obtained from any initial charge composition  $x_{F2}$  lying in regions III and IV. There, extractive composition profiles reach  $SN_{\text{extr},A}$  and are able to cross a rectifying profile that reaches the unstable rectifying node vertex A. Above  $(F_E/V)_{\max,A,R,\infty}$ ,  $SN_{\text{extr},A}$  disappears on the left of  $x_p$ . In contrast, starting from  $x_{F1}$  in regions I and II, all extractive profiles reach  $SN_{\text{extr},B}$  regardless of the entrainer flow rate and enable the recovery of distillate  $x_{DB}$ . Other cases for  $F_E/V > (F_E/V)_{\max,A}$  are detailed in Rodríguez-Donis et al.<sup>30</sup>

The feasible range of operating conditions as feed ratio versus reflux ratio to recover 98 mol % of product is displayed in Figure 12 for chloroform (A) as the distillate and in Figure 13 for vinyl acetate (B) as the distillate.

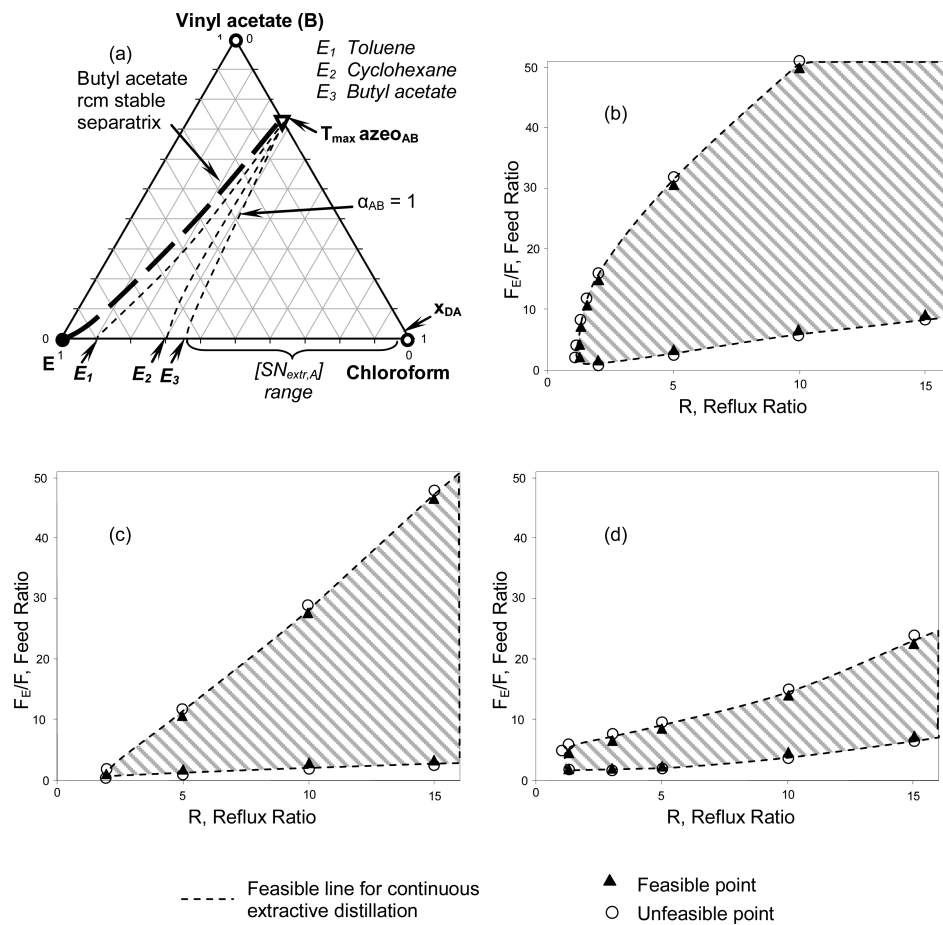


**Figure 13.** Comparison of three different entrainers to recover chloroform (A) from chloroform–vinyl acetate: (a) univolatility curve location and (b) toluene, (c) cyclohexane, and (d) butyl acetate feasible regions.

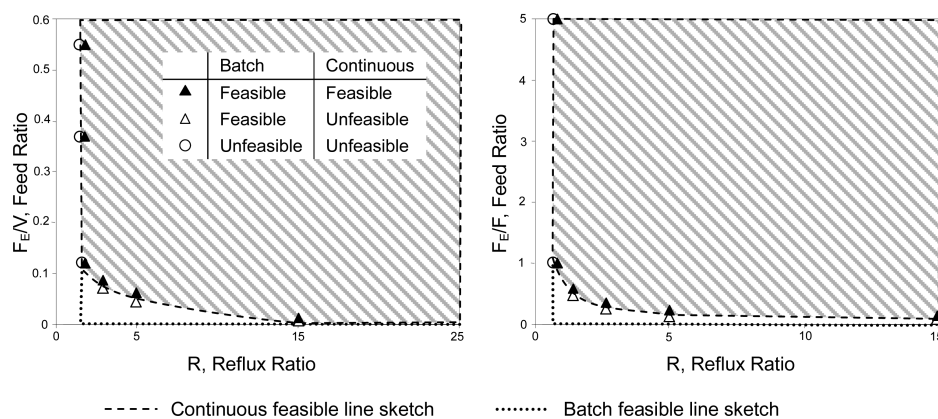


**Figure 14.** Feasibility of batch and continuous extractive distillation of chloroform–vinyl acetate with butyl acetate (class 1.0-2). Feed ratio as a function of the reflux ratio to recover 98 mol % vinyl acetate (B) expressed as a (a) batch or (b) continuous variable.

When chloroform (A) is the distillate (Figure 12), there exists a maximum value for the entrainer/feed flow rate ratio above which both batch and continuous processes are unfeasible. In continuous variable  $F_E/F$ , the maximum gradually decreases as the reflux ratio gets smaller, until a minimum reflux ratio is reached. A detailed calculation of the profile map shows that the feasible region of the rectifying section profiles gets smaller until it can no longer intersect the extractive profile

region.<sup>67</sup> The feasible regions for batch and continuous modes are different, as an additional minimum value of the feed ratio exists for the continuous mode, because, at very low feed ratios, the stripping section can no longer intersect the extractive section.

If the upper limit for the feed flow rate is not a concern for the industrial practice of continuous extractive distillation, the lower limit should be as low as possible to keep the energy

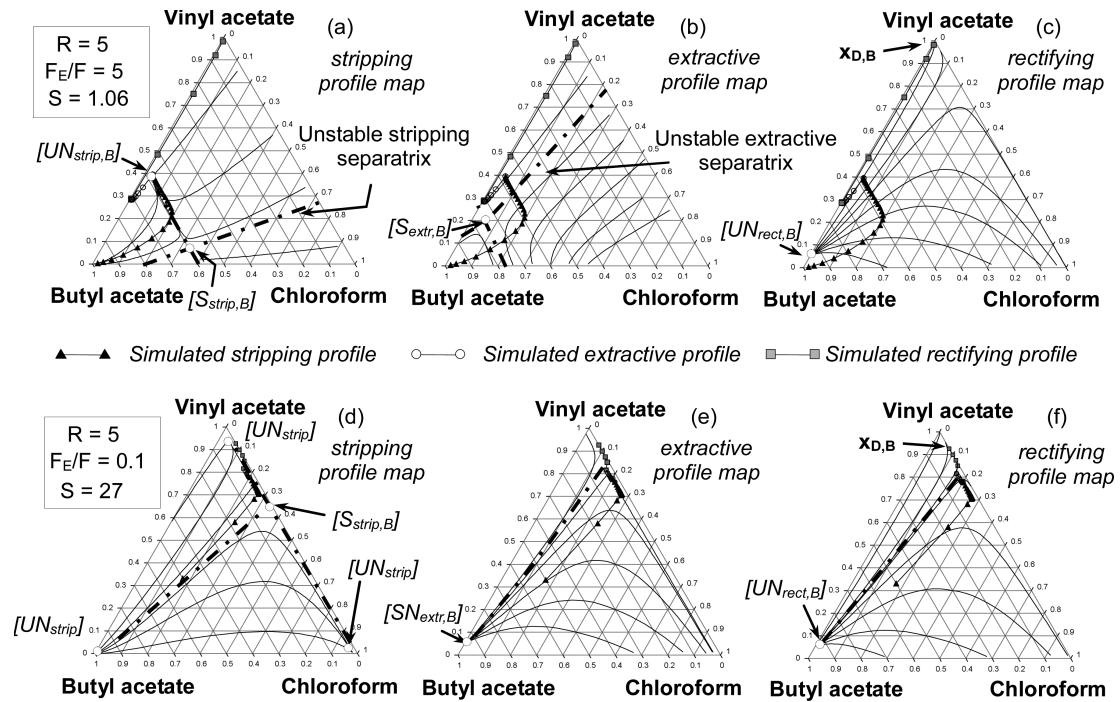


**Figure 15.** Rigorous simulation result to recover vinyl acetate (B) at  $F_E/F = 5$ ,  $R = 5$  and  $F_E/F = 0.1$ ,  $R = 5$ , compared with calculated profiles: (a,d) stripping section, (b,e) extractive section, and (c,f) rectifying section.

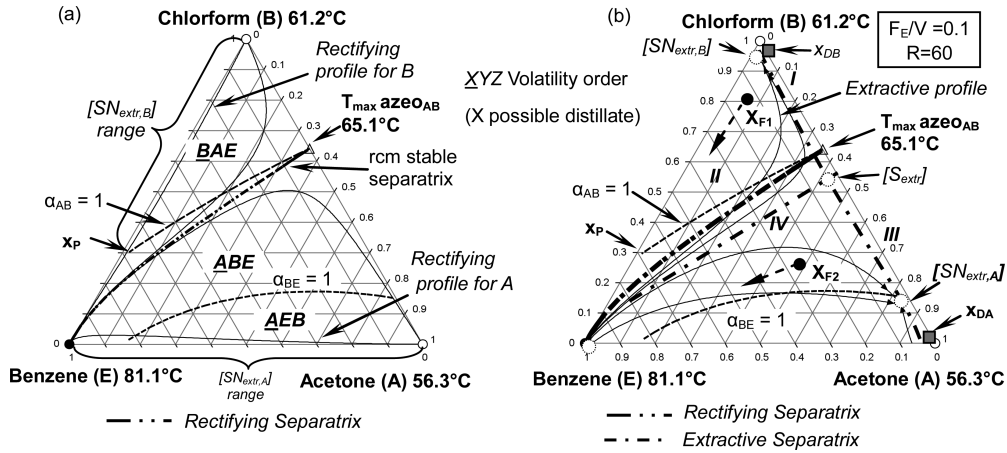


**Figure 16.** Separation of acetone—chloroform using benzene: (a) class 1.0-2 residue curve map (rcm) and batch extractive profile map; (b)  $F_E/V = 0.1$  ( $F_E/V$ )<sub>max</sub>,  $R = 60$ .

demand low. Figure 13 compares three entrainers suitable for the recovery of chloroform as the distillate, under class 1.0-2. The location of the univolatility line is closest to E for toluene, followed by cyclohexane and finally butyl acetate (Figure 13a). This expands the  $SN_{extr,A}$  range, and toluene indeed has the highest upper limit for the entrainer/feed flow rate ratio (Figure 13b), followed by cyclohexane and butyl acetate. The opposite order holds for the order of the lowest limit for the entrainer/feed flow rate ratio. Concerning the reflux ratio, toluene enables operation at the lowest reflux ratio. Overall, Figure 13 indicates that toluene exhibits the largest extractive feasible region, which can result in better operational stability. A definite choice would require more process analysis and optimization.

When vinyl acetate (B) is the distillate, there is no limit for the entrainer/feed flow rate ratio in the batch process (Figure

14). Concerning the reflux ratio, an unstable extractive separatrix reduces the feasible region at low reflux ratio,<sup>30</sup> thus defining an effective minimum feasible value for the reflux ratio, for both batch and continuous modes. Overall, the feasible region is again smaller for the continuous process than for the batch process when the same purity is targeted, because of the additional requirement that the stripping and extractive sections intersect for the continuous process (e.g., below  $F_E/F = 0.2$ ).

A rigorous simulation was carried out with ProsimPlus for an extractive column with the specifications listed in Table 2, and the results are compared in Figure 15 to the approximate composition profile maps. As in the class 1.0-1a case, the shapes of the approximate and rigorous profiles agree well. For the conditions  $F_E/F = 5$  and  $R = 5$ , the process is feasible, as the

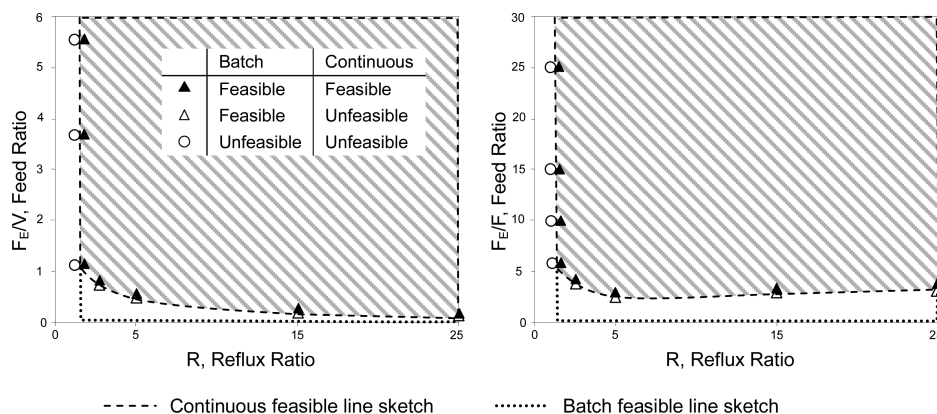


**Figure 17.** Feasibility of batch and continuous extractive distillation of acetone–chloroform with benzene (class 1.0-2). Feed ratio as a function of the reflux ratio to recover 98 mol % acetone (A) expressed as a (a) batch or (b) continuous variable.

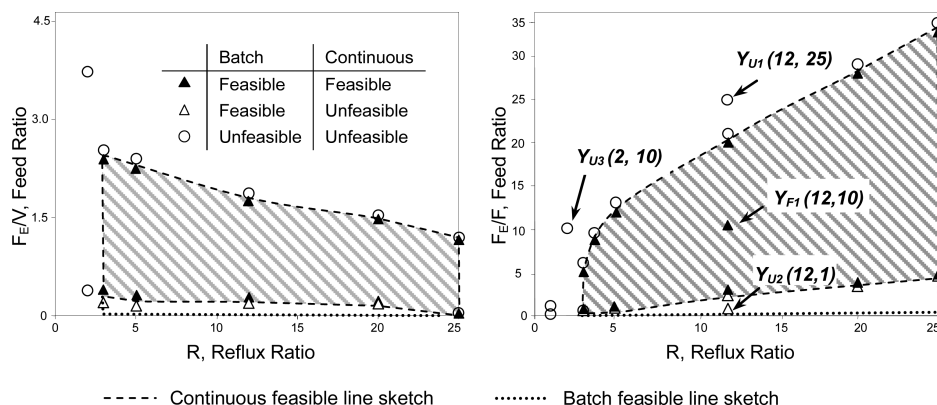


**Figure 18.** Feasibility of batch and continuous extractive distillation of acetone–chloroform with benzene (class 1.0-2). Feed ratio as a function of the reflux ratio to recover 98 mol % chloroform (B) expressed as a (a) batch or (b) continuous variable.

distillate purity reaches 98.2% in vinyl acetate. For the conditions  $F_E/F = 5$  and  $R = 0.1$ , the process is unfeasible, as the distillate purity can reach only 88% in vinyl acetate.

**4.2.2. Class 1.0-2 Case b:  $\alpha_{AB} = 1$  Curve Reaches Binary Side B–E.** Separation of the maximum-boiling azeotrope acetone (A, 56.3 °C)–chloroform (B, 61.2 °C) ( $x_{azeo,A} = 0.37$  at 65.1 °C) by adding heavy entrainer benzene (81.1 °C) illustrates the case when the  $\alpha_{AB} = 1$  curve reaches the side B–E (Figure 16). The criterion for batch extractive processes states that A can be distilled without any limit on the entrainer/feed ratio, whereas there exists a maximum entrainer/feed ratio to obtain B. Depending of the overall feed composition, either A or B can be distilled: From  $x_{F1}$ , B is the distillate product, whereas from  $x_{F2}$  below the extractive separatrix, A is the distillate product.

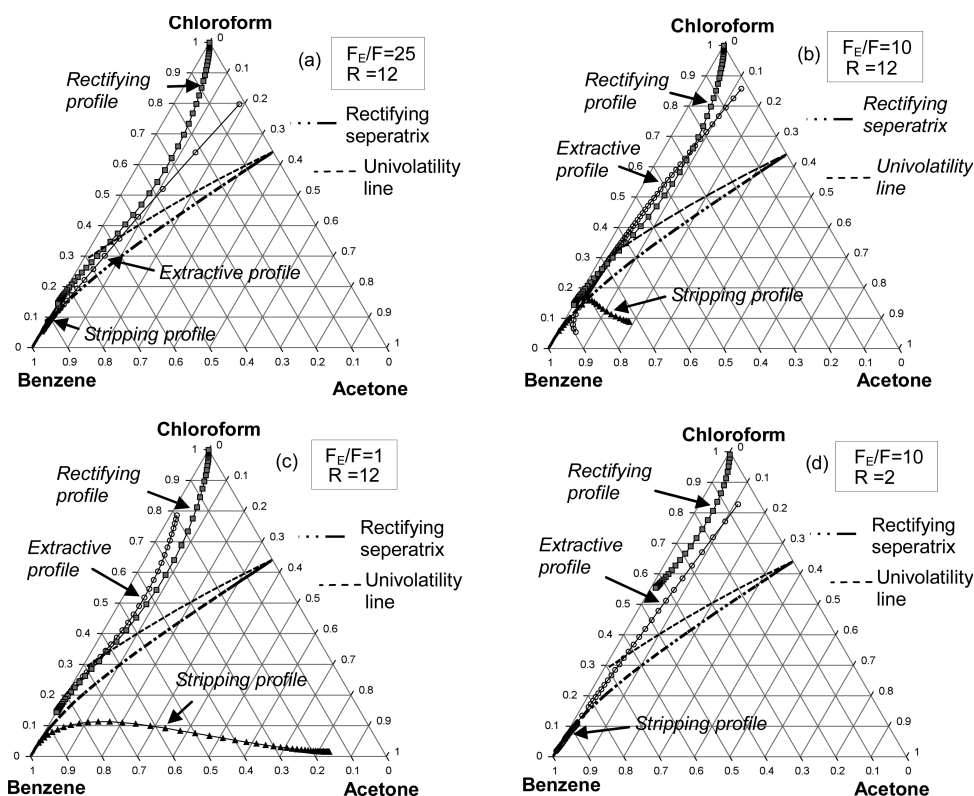
The feasible range of operating conditions as feed ratio versus reflux ratio to recover a product with 98 mol % purity and 98% recovery is displayed in Figure 17 for acetone (A) and in Figure 18 for chloroform (B). Figure 17 is similar to Figure 14 for the previous mixture. Again, the feasible ranges of the batch and continuous processes are different because the continuous process requires that the stripping profile intersect the extractive profile when the same purity is targeted.

Figure 18 for chloroform (B) shows the maximum entrainer/feed ratio value. It is slightly different from that in Figure 12 for the previous mixture, as now the feasible ranges for the batch and continuous processes are different.

Figure 19 displays the composition profiles computed to obtain  $x_D = 0.98$ , under four operating conditions reported in Figure 18b. For  $Y_{U1}$  ( $R = 12$ ,  $F_E/F = 25$ ), the process is unfeasible, as the rectifying profile cannot intersect the extractive section (Figure 19a). For  $Y_{F1}$  ( $R = 12$ ,  $F_E/F = 10$ ), the process is feasible (Figure 19b). For  $Y_{U2}$  ( $R = 12$ ,  $F_E/F = 1$ ), the batch process is feasible, but the continuous process is not because the stripping profile cannot intersect the extractive profile (Figure 19c). Figure 19d is for point  $Y_{U3}$  ( $R = 2$ ,  $F_E/F = 10$ ), for which the reflux ratio is lower than the minimum reflux ratio value: The rectifying profile is so short that it does not intersect the extractive section.

## 5. CONCLUSIONS

A feasibility method originally built for batch extractive distillation processes at infinite reflux ratio was extended to determine the feasible ranges of the operating parameters reflux ratio ( $R$ ) and feed ratio ( $F_E/F$ ,  $F_E/V$ ) for both continuous and batch processes. The first step uses the feasibility criterion for general extractive distillation processes reported by Rodríguez-Donis et al.<sup>30</sup> and requires only the knowledge of the rcm topology and classification, along with the computation of the univolatility line. It predicts the possible products and the existence of limiting values for the entrainer/feed flow rate ratio. Step 2 seeks the feasible ranges of the reflux ratio and entrainer/feed flow rate ratio by checking the intersection of the approximate composition profile in each column section,



**Figure 19.** Rectifying, extractive, and stripping compositions for four operating parameter points taken from Figure 18: (a) point  $Y_{U1}$ , (b) point  $Y_{F1}$ , (c) point  $Y_{U2}$ , and (d) point  $Y_{U3}$ .

depending on the reflux ratio and entrainer/feed flow rate ratio. In step 3, a rigorous simulation confirms the predictions of step 2. Therefore, the approximate calculations are able to evaluate the feasibility of continuous extractive distillation processes under finite-reflux-ratio conditions. They also provide information about the location of pinch points and possible composition profile separatrixes that could impair process feasibility.

For class 1.0-1a (minimum-boiling azeotrope separation A–B by adding heavy entrainer E), two subcases arise depending on whether the univolatility line  $\alpha_{AB} = 1$  intersects the A–E edge (case a) or the B–E edge (case b). For case a (case b), component A (component B) is the distillate product, provided that the entrainer/feed flow rate ratio lies above a minimum value at a given reflux ratio. The minimum value  $F_E/F$  is higher for the continuous process than for the batch process when the same purity is targeted. This is true because the continuous process sets stricter feasible conditions according to which the composition profile of the stripping section must intersect that of the extractive section. Under a finite reflux ratio, an extractive unstable separatrix moves inside the diagram and impacts the feasible composition region, setting a minimum reflux ratio limit.

For class 1.0-2 (maximum-boiling azeotrope separation A–B by adding heavy entrainer E), the univolatility line  $\alpha_{AB} = 1$  can also intersect the A–E edge (case a) or the B–E edge (case b). The general criterion states that, under an infinite reflux ratio, both A and B can be obtained at the top, depending on the overall feed composition location. There also exists a maximum value for  $F_E/F$  for case a (case b) when component A (component B) is the distillate. Under a finite reflux ratio, the

limiting value of  $F_E/F$  holds and is supplemented for the continuous process by a minimum  $F_E/F$  value, because the stripping profile, specifically for the continuous process, must intersect the extractive profile. Again, for both processes, there also exists a minimum reflux ratio.

The methodology also enabled a comparison of three entrainers leading to the same diagram and subcase, in particular, in terms of the extent and size of the ranges of the reflux ratio and the entrainer/feed flow rate ratio.

## AUTHOR INFORMATION

### Corresponding Author

\*E-mail: Vincent.Gerbaud@ensiacet.fr.

### Notes

The authors declare no competing financial interest.

## REFERENCES

- (1) Nakaiwa, M.; Huang, K.; Naito, K.; Endo, A.; Akiya, T.; Nakane, T.; Takamatsu, T. Parameter analysis and optimization of ideal, heat integrated distillation columns. *Comput. Chem. Eng.* **2001**, *25*, 737–744.
- (2) Nakaiwa, M.; Huang, K.; Endo, A.; Ohmori, T.; Akiya, T.; Takamatsu, T. Internally heat-integrated distillation columns: A review. *Chem. Eng. Res. Des.* **2003**, *81* (1), 162–177.
- (3) Skogestad, S. Dynamics and Control of Distillation Columns—A Critical Survey. *MIC J.* **1997**, *18*, 177–217.
- (4) Skogestad, S.; Wittgens, B.; Litto, R.; Sorensen, E. Multivessel batch distillation. *AIChE J.* **1997**, *43* (4), 971.
- (5) Jogwar, S. S.; Baldea, M.; Daoutidis, P. Dynamics and Control of Process Networks with Large Energy Recycle. *Ind. Eng. Chem. Res.* **2009**, *48*, 6087–6097.



- (6) Wolff, E. A.; Skogestad, S. Operation of Integrated Three-Product (Petlyuk) Distillation Columns. *Ind. Eng. Chem. Res.* **1995**, *34*, 2094–2103.
- (7) Halvorsen, I. J.; Skogestad, S. Optimal operation of Petlyuk distillation: Steady-state behavior. *J. Process Control* **1999**, *9*, 407–424.
- (8) Tamayo-Galván, V. E.; Segovia-Hernández, J. G.; Hernández, S.; Hernández, H. Controllability analysis of modified Petlyuk structures. *Can. J. Chem. Eng.* **2008**, *86*, 62–71.
- (9) Halvorsen, I. J.; Skogestad, S. Energy efficient distillation. *J. Nat. Gas Sci. Eng.* **2011**, *3*, 571–580.
- (10) Hilmen, E. K. Separation of azeotropic mixtures: Tools for analysis and studies on batch distillation operation. Ph.D. Thesis, Norwegian University of Science and Technology, Trondheim, Norway, 2000.
- (11) Kiva, V. N.; Hilmen, E. K.; Skogestad, S. Azeotropic Phase Equilibrium Diagrams: A Survey. *Chem. Eng. Sci.* **2003**, *58*, 1903–1953.
- (12) Reshetov, S. A.; Kravchenko, S. V. Statistics of Liquid–Vapor Phase Equilibrium Diagrams for Various Ternary Zeotropic Mixtures. *Theor. Found. Chem. Eng.* **2007**, *41* (4), 451–453.
- (13) Doherty, M. F.; Malone, M. F. *Conceptual Design of Distillation Systems*; McGraw-Hill: New York, 2001.
- (14) Petlyuk, F. B. *Distillation Theory and Its Application to Optimal Design of Separation Units*; Cambridge University Press: Cambridge, U.K., 2004.
- (15) Luyben, W. L.; Chien, I. L. *Design and Control of Distillation Systems for Separating Azeotropes*; Wiley: New York, 2010.
- (16) Repke, J. U.; Klein, A.; Bogle, D.; Wozny, G. Pressure Swing Batch Distillation for Homogeneous Azeotropic Separation. *Chem. Eng. Res. Des.* **2007**, *85*, 492–501.
- (17) Modla, G.; Lang, P. Feasibility of new pressure swing batch distillation methods. *Chem. Eng. Sci.* **2008**, *63* (11), 2856–2874.
- (18) Modla, G. Pressure swing batch distillation by double column systems in closed mode. *Comput. Chem. Eng.* **2010**, *34*, 1640–1654.
- (19) Modla, G.; Lang, P.; Denes, F. Feasibility of separation of ternary mixtures by pressure swing batch distillation. *Chem. Eng. Sci.* **2010**, *65* (2), 870–881.
- (20) Modla, G. Separation of a Chloroform–Acetone–Toluene Mixture by Pressure-Swing Batch Distillation in Different Column Configurations. *Ind. Eng. Chem. Res.* **2011**, *50* (13), 8204–8215.
- (21) Rodríguez-Donis, I.; Gerbaud, V.; Joulia, X. Entrainer Selection Rules for the Separation of Azeotropic and Close Boiling Point Mixtures by Homogeneous Batch Distillation. *Ind. Chem. Eng. Res.* **2001**, *40* (12), 2729–2741.
- (22) Rodríguez-Donis, I.; Gerbaud, V.; Joulia, X. Heterogeneous Entrainer Selection Rules for the Separation of Azeotropic and Close Boiling Point Mixtures by Heterogeneous Batch Distillation. *Ind. Chem. Eng. Res.* **2001**, *40* (22), 4935–4950.
- (23) Rodríguez-Donis, I.; Gerbaud, V.; Joulia, X. Feasibility of Heterogeneous Batch Distillation. *AIChE J.* **2002**, *48*, 1168–1178.
- (24) Skouras, S.; Kiva, V.; Skogestad, S. Feasible Separations and Entrainer Selection Rules for Heteroazeotropic Batch Distillation. *Chem. Eng. Sci.* **2005**, *60* (11), 2895–2909.
- (25) Lang, P.; Modla, G. Generalised method for the determination of heterogeneous batch distillation regions. *Chem. Eng. Sci.* **2006**, *61* (13), 4262–4270.
- (26) Denes, F.; Lang, P.; Modla, G.; Joulia, X. New double column system for heteroazeotropic batch distillation. *Comput. Chem. Eng.* **2009**, *33* (10), 1631–1643.
- (27) Andersen, H. W.; Laroche, L.; Morari, M. Dynamics of homogeneous azeotropic distillation columns. *Ind. Eng. Chem. Res.* **1991**, *30*, 1846–1855.
- (28) Knapp, J. P.; Doherty, M. F. Thermal integration of homogeneous azeotropic distillation sequences. *AIChE J.* **1990**, *36*, 969–983.
- (29) Knapp, J. P.; Doherty, M. F. Minimum Entrainer Flow for Extractive Distillation: A Bifurcation Theoretic Approach. *AIChE J.* **1994**, *40* (2), 243–268.
- (30) Rodríguez-Donis, I.; Gerbaud, V.; Joulia, X. Thermodynamic Insights on the Feasibility of Homogeneous Batch Extractive Distillation. 1. Azeotropic Mixtures with Heavy Entrainer. *Ind. Chem. Eng. Res.* **2009**, *48* (7), 3544–3559.
- (31) Rodríguez-Donis, I.; Gerbaud, V.; Joulia, X. Thermodynamic Insights on the Feasibility of Homogeneous Batch Extractive Distillation. 2. Low-Relative-Volatility Binary Mixtures with a Heavy Entrainer. *Ind. Chem. Eng. Res.* **2009**, *48* (7), 3560–3572.
- (32) Rodríguez-Donis, I.; Gerbaud, V.; Joulia, X. Thermodynamic Insights on the Feasibility of Homogeneous Batch Extractive Distillation. 3. Azeotropic Mixtures with Light Boiling Entrainer. *Ind. Chem. Eng. Res.* **2012**, *51*, 4643–4660.
- (33) Rodríguez-Donis, I.; Gerbaud, V.; Joulia, X. Thermodynamic Insights on the Feasibility of Homogeneous Batch Extractive Distillation. 4. Azeotropic Mixtures with Intermediate Boiling Entrainer. *Ind. Chem. Eng. Res.* **2012**, *51*, 6489–6501.
- (34) Rodríguez-Donis, I.; Gerbaud, V.; Joulia, X. Thermodynamic insight on extractive distillation with entrainer forming new azeotropes. In *Distillation & Absorption 2010*; de Haan, A. B., Kooijman, H., Górak, A., Eds.; Eindhoven University of Technology: Eindhoven, The Netherlands, 2010; pp 431–436.
- (35) Rodríguez-Donis, I.; Papp, K.; Gerbaud, V.; Joulia, X.; Rev, E.; Lelkes, Z. Column Configurations of Continuous Heterogeneous Extractive Distillation. *AIChE J.* **2007**, *53* (8), 1982–1993.
- (36) Steger, C.; Varga, V.; Horvath, L.; Rev, E.; Fonyo, Z.; Meyer, M.; Lelkes, Z. Feasibility of Extractive Distillation Process Variants in Batch Rectifier Column. *Chem. Eng. Process* **2005**, *44*, 1237–1256.
- (37) Frits, E. R.; Lelkes, Z.; Fonyo, Z.; Rev, E.; Markot, M. Cs. Finding Limiting Flows of Batch Extractive Distillation with Interval Arithmetics. *AIChE J.* **2006**, *52* (9), 3100–3108.
- (38) Yatim, H.; Moszkowicz, P.; Otterbein, M.; Lang, P. Dynamic Simulation of a Batch Extractive Distillation Process. *Comput. Chem. Eng.* **1993**, *17*, S57–S62.
- (39) Lang, P.; Yatim, H.; Moszkowicz, P.; Otterbein, M. Batch Extractive Distillation under Constant Reflux Ratio. *Comput. Chem. Eng.* **1994**, *18*, 1057–1069.
- (40) Lelkes, Z.; Lang, P.; Moszkowicz, P.; Benadda, B.; Otterbein, M. Batch extractive distillation: The process and the operational policies. *Comput. Chem. Eng.* **1998**, *22*, 653–656.
- (41) Lelkes, Z.; Lang, P.; Benadda, B.; Moszkowicz, P. Feasibility of Extractive Distillation in a Batch Rectifier. *AIChE J.* **1998**, *44*, 810–822.
- (42) Wahnschafft, O. M.; Koehler, J. W.; Blass, E.; Westerberg, A. W. The Product Composition Regions of Single-Feed Azeotropic Distillation Columns. *Ind. Eng. Chem. Res.* **1992**, *31*, 2345–2362.
- (43) Fidkowski, Z. T.; Doherty, M. F.; Malone, M. F. Feasibility of Separations for Distillation of Nonideal Ternary Mixtures. *AIChE J.* **1993**, *39* (8), 1303–1321.
- (44) Pöllmann, P.; Blass, E. Best Products of Homogeneous Azeotropic Distillations. *Gas Sep. Purif.* **1994**, *8*, 194–228.
- (45) Levy, S. G.; Van Dongen, D. B.; Doherty, M. F. Design and Synthesis of Homogeneous Azeotropic Distillation: 2. Minimum Reflux Ratio Calculations for Nonideal and Azeotropic Columns. *Ind. Eng. Chem. Fundam.* **1985**, *24*, 463–474.
- (46) Doherty, M. F.; Calderola, G. A. Design and synthesis of homogeneous azeotropic distillations. 3. The sequencing of columns for azeotropic and extractive distillations. *Ind. Eng. Chem. Fundam.* **1985**, *24* (4), 474–485.
- (47) Bausa, J. R.; Watzdorf, V.; Marquardt, W. Shortcut methods for nonideal multicomponent distillation: 1. Simple columns. *AIChE J.* **1998**, *44*, 2181–2198.
- (48) Urdaneta, R. Y.; Bausa, J.; Bruggemann, S.; Marquardt, W. Analysis and conceptual design of ternary heterogeneous azeotropic distillation processes. *Ind. Eng. Chem. Res.* **2002**, *41*, 3849–3866.
- (49) Laroche, L.; Bekiaris, N.; Andersen, H. W.; Morari, M. Homogeneous Azeotropic Distillation: Comparing Entrainers. *Can. J. Chem. Eng.* **1991**, *69*, 1302–1319.

- (50) Laroche, L.; Bekiaris, N.; Andersen, H. W.; Morari, M. The Curious Behavior of Homogeneous Azeotropic Distillation—Implications for Entrainer Selection. *AIChE J.* **1992**, *38*, 1309–1328.
- (51) Lang, P.; Modla, G.; Benadda, B.; Lelkes, Z. Homoazeotropic Distillation of Maximum Azeotropes in a Batch Rectifying Column with Continuous Entrainer Feeding. I. Feasibility Studies. *Comput. Chem. Eng.* **2000**, *24*, 1665–1671.
- (52) Lang, P.; Modla, G.; Kotai, B.; Lelkes, Z.; Moszkowicz, P. Homoazeotropic Distillation of Maximum Azeotropes in a Batch Rectifying Column with Continuous Entrainer Feeding. II. Rigorous Simulation Results. *Comput. Chem. Eng.* **2000**, *24*, 1429–1435.
- (53) Levy, S. G.; Doherty, M. F. Design and synthesis of homogeneous azeotropic distillations. 4. Minimum reflux ratio calculations for multiple-feed columns. *Ind. Eng. Chem. Fundam.* **1986**, *25* (2), 269–279.
- (54) Wahnschafft, O. M.; Westerberg, A. W. The Product Composition Regions of Azeotropic Distillation Columns: II. Separability in Two-Feed Columns and Entrainer Selection. *Ind. Eng. Chem. Res.* **1993**, *32*, 1108–1120.
- (55) Van Dongen, D. B.; Doherty, M. F. Design and Synthesis of Homogeneous Azeotropic Distillations: 1. Problem Formulation for a Single Column. *Ind. Eng. Chem. Fundam.* **1985**, *24*, 454–463.
- (56) Doherty, M. F.; Knapp, J. P. Distillation, Azeotropic, and Extractive Distillation. In *Kirk-Othmer Encyclopedia of Chemical Technology*; John Wiley & Sons: New York, 2004; pp 1580–1585.
- (57) Brüggemann, S.; Marquardt, W. Shortcut Methods for Nonideal Multicomponent Distillation: 3. Extractive Distillation Columns. *AIChE J.* **2004**, *50*, 1129–1149.
- (58) Kossack, S.; Kraemer, K.; Gani, R.; Marquardt, W. A systematic synthesis framework for extractive distillation processes. *Chem. Eng. Res. Des.* **2008**, *86* (7A), 781–792.
- (59) Lucia, A.; Amale, A.; Taylor, R. Distillation pinch points and more. *Comput. Chem. Eng.* **2008**, *32*, 1350–1372.
- (60) Petlyuk, F.; Danilov, R.; Skouras, S.; Skogestad, S. Identification and analysis of possible splits for azeotropic mixtures. 1. Method for column sections. *Chem. Eng. Sci.* **2011**, *66*, 2512–2522.
- (61) Petlyuk, F.; Danilov, R.; Skouras, S.; Skogestad, S. Identification and analysis of possible splits for azeotropic mixtures. 2. Method for simple columns. *Chem. Eng. Sci.* **2012**, *69* (1), 159–169.
- (62) Hilmen, E. K.; Kiva, V. N.; Skogestad, S. Topology of Ternary VLE Diagrams: Elementary Cells. *AIChE J.* **2002**, *48* (4), 752–759.
- (63) *ProsimPlus 3.1*; ProSim: Labège Cedex, France, 2009. User guide available at <http://www.prosim.net> (accessed Feb 2012).
- (64) *Aspen Plus 11.1 User Guide*; AspenTech: Cambridge, MA, 2001. Available at <http://www.aspentech.com> (accessed Feb 2012).
- (65) Luyben, W. L. Effect of Solvent on Controllability in Extractive Distillation. *Ind. Eng. Chem. Res.* **2008**, *47*, 4425–4439.
- (66) Luyben, W. L. Comparison of Extractive Distillation and Pressure-Swing Distillation for Acetone–Methanol Separation. *Ind. Eng. Chem. Res.* **2008**, *47*, 2696–2707.
- (67) Shen, W. Extension of thermodynamic insights on batch extractive distillation to continuous operation. Ph.D. Thesis, Institut National Polytechnique de Toulouse, Toulouse, France, 2012.